Accepted Manuscript

Family wide analysis of aminoacyl-sulfamoyl-3-deazaadenosine analogues as inhibitors of aminoacyl-tRNA synthetases

Baole Zhang, Steff De Graef, Manesh Nautiyal, Luping Pang, Bharat Gadakh, Matheus Froeyen, Lieve Van Mellaert, Sergei V. Strelkov, Stephen D. Weeks, Arthur Van Aerschot

PII: S0223-5234(18)30135-1

DOI: 10.1016/j.ejmech.2018.02.013

Reference: EJMECH 10190

To appear in: *European Journal of Medicinal Chemistry*

Received Date: 6 December 2017

Revised Date: 5 February 2018

Accepted Date: 6 February 2018

Please cite this article as: B. Zhang, S. De Graef, M. Nautiyal, L. Pang, B. Gadakh, M. Froeyen, L. Van Mellaert, S.V. Strelkov, S.D. Weeks, A. Van Aerschot, Family wide analysis of aminoacyl-sulfamoyl-3-deazaadenosine analogues as inhibitors of aminoacyl-tRNA synthetases, *European Journal of Medicinal Chemistry* (2018), doi: 10.1016/j.ejmech.2018.02.013.

Graphical Abstract:

Family wide analysis of aminoacyl-sulfamoyl-3-deazaadenosine analogues as inhibitors of aminoacyl-tRNA synthetases

Baole Zhang[1 #], Steff De Graef[2 #], Manesh Nautiyal[1], Luping Pang[1,2], Bharat Gadakh[1], Matheus Froeyen[1], Lieve Van Mellaert[3], Sergei V. Strelkov[2], Stephen D. Weeks[2,∞] and Arthur Van Aerschot[1,∞,*]

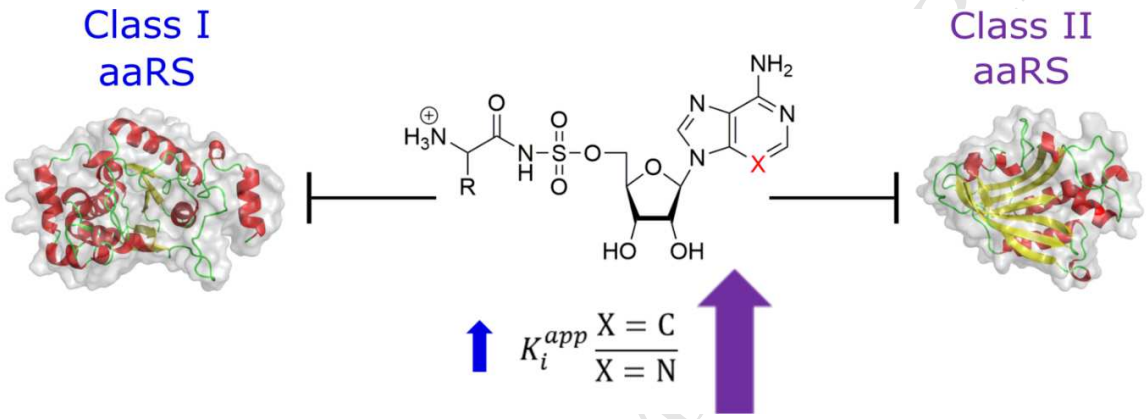

Family wide analysis of aminoacyl-sulfamoyl-3-deazaadenosine analogues as inhibitors of aminoacyl-tRNA synthetases

Baole Zhang[1 #], Steff De Graef[2 #], Manesh Nautiyal[1], Luping Pang[1,2], Bharat Gadakh[1], Matheus Froeyen[1], Lieve Van Mellaert[3], Sergei V. Strelkov[2], Stephen D. Weeks[2,∞] and Arthur Van Aerschot[1,∞,*]

[1] Medicinal Chemistry, Rega Institute for Medical Research, Herestraat 49 box 1041, B-3000 Leuven, Belgium
[2] Laboratory for Biocrystallography, Department of Pharmaceutical and Pharmacological Sciences, Herestraat 49 box 822, B-3000 Leuven, Belgium
[3] Laboratory Molecular Bacteriology, Rega Institute for Medical Research, Herestraat 49 box 1037, B-3000 Leuven, Belgium

* To whom correspondence should be addressed. Tel: +32 16 37 26 24; Fax: +32 16 33 73 40; Email: arthur.vanaerschot@kuleuven.be

[#] These authors contributed equally to this work.

∞ Both authors equally supervised and gave guidance to this work

ABSTRACT

Aminoacyl-tRNA synthetases (aaRS) are enzymes that precisely attach an amino acid to its cognate tRNA. This process, which is essential for protein translation, is considered a viable target for the development of novel antimicrobial agents, provided species selective inhibitors can be identified. Aminoacyl-sulfamoyl adenosines (aaSA) are potent orthologue specific aaRS inhibitors that demonstrate nanomolar affinities in vitro but have limited uptake. Following up on our previous work on substitution of the base moiety, we evaluated the effect of the N^3-position of the adenine by synthesizing the corresponding 3-deazaadenosine analogues (aaS3DA). A typical organism has 20 different aaRS, which can be split into two distinct structural classes. We therefore coupled six different amino acids, equally targeting the two enzyme classes, via the sulfamate bridge to 3-deazaadenosine. Upon evaluation of the inhibitory potency of the obtained analogues, a clear class bias was noticed, with loss of activity for the aaS3DA analogues targeting class II enzymes when compared to the equivalent aaSA. Evaluation of the available crystallographic structures point to the presence of a conserved water molecule which could have importance for base recognition within class II enzymes, a property that can be explored in future drug design efforts.

1. Introduction

Infectious diseases are the second largest cause of mortality worldwide [1]. In 2015, an estimated 9.3 million people died as result of microbial infection, surpassing the number of deaths caused by cancer [2]. Critically, our most important weapons against such pathogens have become less effective because of the rise of antimicrobial resistance [3]. This has led to predictions that the deaths associated to infectious diseases will dramatically increase if no immediate action is taken [4]. As part of a global effort to curtail this crisis it has been recommended that new antimicrobials are developed.

Most organisms provide numerous viable targets for new compounds, yet the majority are poorly exploited. The aminoacyl-tRNA synthetase (aaRS) family is one such group that has recently garnered more attention for the development of candidate small molecule inhibitors [5].

Aminoacyl-tRNA synthetases are essential enzymes, found in all cellular life, that play a central role in the translation of the genetic code [6]. They catalyze a two-step process that results in the attachment of a specific amino acid (aa) to its cognate tRNA (**Fig 1. A**). In the first step an aaRS forms a high affinity mixed phosphoanhydride, the aminoacyl-adenylate intermediate (aa-AMP; **Fig 2. a**), from an amino acid and an ATP molecule, yielding pyrophosphate as a byproduct (**Fig 1. A**). In the subsequent step the intermediate carbonyl undergoes a nucleophilic attack from a hydroxyl group from the 3'-terminal ribose of the tRNA, yielding the aminoacylated tRNA product and AMP [7].

A typical organism contains 20 different aaRS, one for each proteinogenic amino acid. Reflecting on their evolutionary origins these can be divided, almost equally, into two distinct classes based on the structure of the catalytic site (**Fig 1. B**). Class I representatives contain the βαβ Rao-Rossman fold commonly observed in nucleotide binding proteins [8]. Sequence analysis has shown that within this domain, all class I orthologues present a highly conserved HIGH and a KMSKS sequence (where each letter corresponds to the amino acid one letter code) [4]. These two motifs, both involved in ATP binding and activation, sandwich the primary sequence of the catalytic domain. The HIGH-motif is found in the first α-helix of the common core structure, while the KMSKS sequence occurs in the C-terminus of this domain in a loop that bridges the catalytic core to the anticodon binding domain. All class II orthologues share a central six-stranded curved β-sheet surrounded by a variable number of α-helices (**Fig 1.B**). Contrasting with the class I aaRS, analysis of class II sequences has identified three cryptic motifs shared amongst members of this family [9]. The first motif is involved in homo-dimerization, a common quaternary arrangement shared amongst class II aaRS, whereas the remaining are necessary for ATP binding and formation of the intermediate [10].

Targeting aaRS is advantageous as these enzymes meet various criteria for modern antibacterial drug discovery [11]. Nature itself has already come up with aaRS inhibitors, such as ileRS inhibitor mupirocin (**Fig 2. c**) and aspRS inhibitor microcin C (**Fig 2. d**). Unfortunately, as with other antibacterial agents that act on a single enzyme target, aaRS inhibitors possess an intrinsic resistance liability [12], and the occurrence of clinical isolates of *S. aureus* that are resistant to mupirocin has been reported [13]. Randall et al. demonstrated that simultaneous targeting of two aaRS enzymes overcomes the resistance liabilities associated with inhibitors acting against a single enzyme [14]. Therefore, it is of considerable interest to identify new compounds that target different orthologues within this family. The simplest approach would be to employ a general scaffold, where simply changing the attached amino acid would expand the portfolio of target aaRS.

Replicating biology, one approach to rationally design aaRS inhibitors is to mimic the aa-AMP intermediate [15]. Most non-hydrolysable aa-AMP analogues reported so far are based on replacing the labile acyl-phosphate linkage of the intermediate with stable bioisosteres such as alkylphosphites

[16-18], esters [19-21], amides [19], hydroxamates [19-21], sulfamates [17, 18, 22-25], sulfamides [17], N-alkoxysulfamides [26] and N-hydroxysulfamides [26]. Among these molecules the aminoacyl-sulfamate (aaSA) analogues (**Fig 2. b)** have proven to be the most potent inhibitors, with improved hydrolytic stability compared to aminoalkyl and aminoacyl-adenylate [27].

However, while the aaSA scaffold has been useful for structural studies of aaRS, their potential as lead compounds for drug development has been hampered by their lack of selectivity and in vivo efficacy [27, 28]. One suggested approach to resolve this problem is to replicate the Trojan-horse strategy employed by some of the natural aaRS antibiotics, attaching such active moieties to bacterial uptake modules that are then released in the cytoplasm by host enzymatic processing [29]. Unfortunately, coupling of the aaSAs to such carriers is limited as the sulfamate group has been reported to be hydrolytically unstable under certain chemical conditions. This is due to the nucleophilic attack of the N^3 of the base on the 5'-leaving moiety resulting in a N^3, C5'-cycloadenosine (**Fig 2. e)** [30]. To resolve this issue we have investigated employing alternative base moieties, with varying success in the resultant inhibitory activity [31]. Building upon these efforts, we report here the synthesis and evaluation of stable 3-deazaadenosine analogues (aaS3DA, **Fig 2. f**). To fully assess the consequence of substituting this single atom in aaSA we have performed a comprehensive family wide analysis of the compounds, synthesizing and evaluating aaS3DA analogues that target both class I and class II aaRS representatives.

2. Results

2.1. Synthesis of aminoacyl-sulfamoyl 3-deazaadenosine analogues

The synthesis of 3-deazaadenosine **7** from cheap and readily available 3,4-diaminopyridine **1** is shown in **Scheme 1**. Cyclization of both amines using triethyl orthoformate and formic acid to afford compound **2** was followed by oxidation to the *N*-oxide **3**. Chlorination with phosphorus oxychloride gave **4** with concomitant reduction of the N-oxide [32]. The heterocyclic base **4** was further reacted with tetra-*O*-acetyl ribofuranose using stannic chloride followed by deprotection of the acetyl moieties using methanolic ammonia to give the 4-chloro nucleoside analogue **6** [33]. Nucleophilic displacement of the chloride using ammonia in methanol at 65 °C did not afford the desired amine **7** while this method works well for the 6-chlorinated purine. This problem was overcome by a nucleophilic displacement with hydrazine followed by reduction with Raney Nickel to yield **7** [34].

Selective sulfamoylation at the primary hydroxyl moiety required prior protection of both secondary alcohol groups. Hereto, formation of the acetonide compound **8** was accomplished with *p*-toluenesulfonic acid in a mixture of anhydrous acetone and 2 equiv. of 2, 2-dimethoxypropane [35]. Direct sulfamoylation of **8** with sulfamoyl chloride followed by aminoacylation led to the synthesis of base-aminoacylated compound **10** (see supplementary file) [36, 37].

Hence, following an established protocol, successful benzoylation of **8** afforded compound **11** [38]. Subsequent reactions with sulfamoyl chloride and hydroxysuccinimide activated esters afforded compounds **12** and **13a-f**, respectively (**scheme 2**). Treatment with sodium methoxide gave compounds **14a-f** [39], and removal of the *tert*-butyloxycarbonyl and acetonide groups was accomplished simultaneously by treating with TFA/water (5:2) to afford **15a-f** [31]. For compounds **15b** and **15c,** the benzyl moieties were removed by treatment with hydrogen in methanol under palladium catalysis right before the final deprotection. In total six aaS3DA compounds were successfully produced. Three of these compounds (**15b, 15e** and **15f**) target class I aaRS and the remaining ones (**15a, 15c** and **15d**) target class II enzymes. All compounds synthesized in this project were unambiguously characterized by ^{1}H, ^{13}C NMR spectroscopy and ESI-MS, except the intermediates **13b-f** and **14b-f** that were only corroborated by ESI-MS.

2.2. Inhibitory activity in *E. coli* S30 extracts

The aaS3DA compounds were evaluated for their ability to inhibit aaRS catalyzed aminoacylation of tRNA in whole cell extracts (**Fig. 3**). As a positive control, the comparative activity was assessed in parallel with the canonical aaSA intermediate analogues. Reactions were performed using a S30 extract from the wild-type *E. coli* K-12 BW28357 strain preincubated with 2.5 µM of each compound. In comparison to their aaSA equivalents, the six aaS3DA analogues showed a clear aaRS class dependent difference in inhibitory activity (**Fig. 3**). For the class I aaRS (ileRS, leuRS and tyrRS), the aaS3DA compounds demonstrated a similar reduction of the enzymatic activity as the adenosine containing compounds (ileSA, leuSA and tyrSA). The amount of inhibition varied between the different aaRS, from a reduction of almost 90% of the extract activity when preincubated with leuS3DA to a significant 40-50% reduction in catalysis with ileS3DA and tyrS3DA. In contrast the aaS3DA compounds demonstrated no, or severely limited, inhibitory activity when tested against the corresponding class II enzymes (aspRS , glyRS and serRS), while the aaSA analogues showed potencies equivalent to earlier reports [27].

2.3. Measurement of in vitro inhibitory activity with purified *E. coli* aaRS

To investigate further whether the observed difference in the class dependent inhibitory activity of the aaS3DA compounds was a result of substitution of the N^3 atom in the base, rather than an effect of extract mediated modification or aberrant binding of the compounds to other proteins in the clarified lysate, the aaS3DA analogues were also evaluated with the corresponding isolated aaRS. Using serial dilutions of the synthesised compounds comparative dose-response curves were generated for each aaSA and aaS3DA pair (**Fig. 4**). These curves were then fitted using the Greco-Hakala equation for high affinity binders to determine the K_i^{app} for each compound (**Table 1**).

In the presence of 500 µM ATP all class I targeting aaS3DA compounds demonstrated sub-micromolar K_i^{app} values (**Fig. 4 A and Table 1**). Relative to aaSA the 3-deazaadenosine containing compounds showed reduced inhibitory activity, but to varying degrees depending on the aaRS. In the worst case, with ileRS, substitution of the N^3 resulted in a 110-fold increase in the K_i^{app}. For leuRS and tyrRS the effect was less pronounced, where the aaS3DA analogues were 4.7 and 10.2 times less active than the analogous aaSA, respectively. In contrast introduction of 3-deazaadenosine into the aminoacyl-sulfamate scaffold had a more dramatic effect on the three compounds targeting class II aaRS, despite the aaSA equivalents demonstrating a range of K_i^{app} values similar to those seen for the class I enzymes (**Fig.4 B and Table 1**). In particular, at the highest concentration tested (2 µM) glyS3DA showed no inhibitory activity against glyRS. Similarly, the aspS3DA and serS3DA compounds were also negatively affected, showing a respective increase in K_i^{app} of 486 and 2900-fold when compared to aspSA and serSA (**Table 1**). The observed aaRS class dependent reduction of inhibitory activity for the aaS3DA compounds, when compared to analogous aaSA, in this assay is in accordance with the above results in cell extracts.

2.4. Antibacterial activity measurements

The obtained target compounds were evaluated for their in vitro antibacterial activity against Gram-positive bacterial strains (*Staphylococcus aureus* ATCC 6538P, *Staphylococcus epidermidis* RP62A and *Kocuria rhizophila* ATCC 9341 (formerly *Sarcina lutea*)), Gram-negative strains (*Escherichia coli* NCIB 8743 and *Pseudomonas aeruginosa* PAO1) and one yeast species (*Candida albicans* CO11) using the broth dilution method. Serial dilutions, from 100 µM to 0.39 µM, of each aaS3DA compound were tested. Unfortunately, none of the compounds demonstrated growth inhibition, even at the maximum concentration tested (data not shown), behaving similarly to what was previously reported for the aaSA equivalents [40].

2.5. Quantum calculation of the electrostatic potential of 3-deazaadenisone

To assess the influence of the removal of the N^3-nitrogen on the electron distribution in 3-deazaadenosine, quantum chemical calculations were performed for adenine and 3-deazaadenine using a N^9-methylated derivative as a substitute for the ribose (**Fig. 5 A** and **B**). The calculations suggest that although the *p*-orbital electrons are similarly delocalised, there is a clear loss of electronegativity at the position where the N^3 is substituted. In addition, the calculated structures show the N^6 and both hydrogens to be coplanar with the purine ring, while for 3-deazaadenine the equivalent hydrogens are found out of plane. This illustrates that in adenine, the N^6 has more sp2 character, in contrast with a larger sp3 hybridization character seen for the N^6 in 3-deazaadenine. This change is reflected in a predicted rise in the pKa of this amine group and an increased nucleophilicity for the 3-deaza congener. This observation is in good agreement with the observed reactivity of the N^6-group during primary coupling of the amino acid to the sulfamate, and the need to use an alternative approach employing the N^6-benzoyl protecting group (**Scheme 2**).

2.6. Bioinformatic analysis

To understand in more detail the apparent class based difference of aaS3DA activity we performed a structure based alignment of all aaRS members in *E. coli* and the gram-positive bacterium *S. aureus*. For some orthologues high resolution X-ray structures are available of the enzyme bound to their respective aaSA. These permitted the identification of crucial residues involved in base recognition that could be extrapolated to the other members in the alignment. In the case of the class I aaRS the adenine moiety is sandwiched between the HIGH containing α-helix and a residue that is typically non-polar, found in most class I aaRS 5-6 residues upstream of the conserved KMSKS loop (**Fig. 5 C, and Supplementary movie**). The bulk of the interaction of the base with the active site appears to be driven by Van der Waals forces. Only two polar interactions with the base are consistently observed in different aaRS:aaSA complex structures, mediated by the interaction of the protein backbone atoms with the N^1 and N^6 position of adenine. Crucially the N^3-atom makes no clear interactions with the protein supporting the described biochemical results.

In stark contrast, the adenosine makes numerous interactions with active site residues in the class II aaRS (**Fig. 5 D and Supplementary movie**). One face of the base makes a π/π interaction with a conserved phenylalanine (or rarely tyrosine) residue, found in the class wide motif-2, while the opposite face of this heterocycle interacts with a highly conserved arginine residue present in the structurally preserved α-helix of motif-3 via cation/π bonding. In addition to these weak interactions N^1, N^3 and N^6 all make H-bond interactions with conserved features shared amongst all class II aaRS members. Both the N^1 and N^6 make polar interactions with backbone atoms of a poorly conserved residues in motif-2, similarly to that seen in the class I enzymes. In addition, the N^6-amine also interacts with a highly conserved acidic residue within the same motif (**Fig. 5 D and Supplementary movie**). Crucially, the N^3 interacts with the protein via a water molecule, typically positioned 3 Å away, that is found capping the N-terminus of the conserved α-helix of motif-3 (**Fig. 5 D and Supplementary movie**). This water is held in place by interactions with protein backbone amines and a conserved side chain interaction.

As the QM calculations suggest a loss of negative electrostatic potential in the 3-deazaadenosine compounds at the position of substitution, it is thus likely that the reduction of K_i^{app} observed for the class II targeting aaS3DA (**Figs. 3** and **4**) is principally a result of a loss of interaction with water. The absence of this interaction, further modified by steric interference of the water with the proton on C^3 could result in repositioning of the aaS3DA base in the active site such that the additional H-bond interactions are also destabilised leading to the dramatic reduction in inhibitory activity observed for these compounds.

3. Discussion

Non-hydrolysable aa-AMP analogues potently inhibit aaRS in vitro, with nanomolar range affinities, yet they are devoid of antibacterial activity due to limited uptake [27, 28]. One approach to overcome this problem is to extend the mimicry of natural compounds (e.g. **Fig. 2 d**), by coupling these

enzymatic intermediate equivalents to an uptake module such as a peptide or a siderophore. To simplify the synthesis of such complex molecules it is essential to reduce the number of reactive groups present in the inhibitor without comprising activity or negatively affecting translocation of the compound into the cell. In this work we investigated the effect of replacement of the N^3 of adenine in the aaSA scaffold, a modification predicted to enhance chemical stability, on the activity of the resultant compounds [35].

There is a clear precedent in the synthesis and application of deazapurines in medicinal chemistry [41]. In particular compounds containing 3-deazadenosine have been successfully introduced into a number of antibacterials. C. Shi et al reported the successful synthesis of 5'-*O*-[*N*-(biotinyl)sulfamoyl]-3-deazaadenosine, a compound that inhibits the biotin protein ligase birA, a global regulator of fatty acid biosynthesis in mycobacterium [35]. Competitive affinity measurements demonstrated that this compound had a similar K_D to the adenosine analog, and possessed equivalent antitubercular activity, with an MIC of 1.56 μM. In addition, the chemical stability of this compound was also increased when compared to the adenine containing equivalent [30]. In contrast, the same research group also reported 5'-*O*-[*N*-(salicyl)sulfamoyl]-2-aryl-8-aza-3-deazaadenosine analogues as bispecific compounds designed to block siderophore biosynthesis in *Mycobacterium tuberculosis* by inhibiting the adenylating enzyme MbtA [42]. Unfortunately, the combination of 8-aza and 3-deaza in the base at same time increased the apparent K_i by 30 fold, when compared to the equivalent conjugated adenine, and increased the MIC greater than 500 fold, despite the compound demonstrating enhanced chemical stability. These discrepancies point to need for a thorough evaluation of equivalent deazapurines to fully understand their SAR properties.

To obtain a broader understanding of the implications of replacing the N^3 of adenine in the potent aaSA compounds we synthesized six aminoacyl-sulfamoyl-3-deazaadenosine analogues. As the aaRS family is divided into two specific structural subclasses [10], we specifically created three aaS3DA compounds targeting representatives from each group. For the class I aaRS we chose ileRS, leuRS and tyrRS as targets for the aaS3DA analogues as the attached amino acid demonstrate low solubility and thus could improve the drug-like qualities of the resultant products. For the class II targeting aaS3DA we picked aspRS, serRS and glyRS as the attached amino acids extending the chemical profile under evaluation from acidic and polar, and to the simple unbranched glycine. The approach used varied from that previously reported [35], by direct ring closure of 3,4-diamino-pyridine and subsequent chlorination of the N-oxide, overall providing a shorter and higher yielding route to construct the 3-deaza adenine heterocycle. (**Scheme 1**).

The activity of all six aaS3DA compounds were evaluated by determining their ability to prevent a full catalytic cycle of each enzyme, measuring the final transfer of the activated amino acid to tRNA (**Fig.1 A**). For completeness, these measurements were performed in an *E. coli* whole cell extract as well as with the isolated enzymes. In the cell lysates the aaS3DA intermediate mimics targeting class I aaRS demonstrated inhibitory activity similar to the parent aaSA molecule. With the purified enzymes there was a measurable increase in K_i^{app} for all three class I aaS3DAs, with ileS3DA

showing the largest increase in this value, over 100-fold, when compared to ileSA (**Fig. 4 and Table 1**). Ultimately, the measured K_i^{app} values were still sub-micromolar, below the concentration tested in the cell extracts, explaining the observed comparable potency of the class I targeting aaS3DA and aaSA in this complex system. Surprisingly however, for class II targeted enzymes the inhibitory activity in cell extracts of the aaS3DA was almost completely lost upon removal of the N^3-position. This class bias was further confirmed in assays with the purified aaRS, where all tested compounds demonstrated an increase in their Ki^{app} relative to the equivalent aaSA (**Table 1**). This raising of the K_i^{app}, varying from 500-fold for aspS3DA to 4000-fold for serS3DA, was significantly higher than that observed for even the most affected class I targeting aaS3DA.

To further understand how the aaRS class dependent selectivity of the 3-deazaadenosine analogues is manifested we performed QM chemical calculations to determine changes to the electrostatic potential of the base. Overall, the p-orbital electrons are similarly delocalised in 3-deazaadenine and adenine, but there is a clear loss of electronegativity at the substituted 3-carbon position in the former compound. This principle difference therefore likely dictates the observed aaRS class specificity. A detailed structural and bioinformatics analysis of the two classes point to quite distinct mechanisms of base recognition in terms of the whole heterocycle but, more importantly, points to a key difference between the enzyme groups in terms of identifiable N^3 interactions (**Fig. 5**). Specifically, the presence of a conserved water molecule at a position where it can engage in hydrogen bonding between the N^3 of the aaS3D, is a conserved feature in the class II enzymes. At present though how the loss of this single interaction results in a dramatic increase in the apparent K_i of the aaS3DA analogues that target class II aaRS is not clear, and requires further biophysical investigation.

In addition to demonstrating that the aaS3D analogues can be successfully employed to inhibit class I aaRS, the combined results could be useful in the future design of novel inhibitors. In particular the single atom substitution performed here has highlighted key differences in the pharmacophores between the two aaRS classes that could be exploited. Previously our group investigated the importance of adenine in ileSA by replacing it with other natural nucleobases. Surprisingly, substitution of this conserved purine with a pyrimidine resulted in an increase in inhibitory activity of the synthesised compounds in an S30 extract [31]. This observation is in agreement with the results of this study, which shows that class I tRNA aaRS make a minimal number of interactions with the base, and suggests that this moiety can be readily replaced. This hypothesis is supported by examination of the structure of mupirocin (**Fig 2 C**), a natural ileRS inhibitor, which presents a conjugated system with an ester function in place of adenine. Diverging from this, the class II aaRS offer multiple modes of interaction with the base, a property that could be explored for developing high affinity compounds.

4. Conclusion

Large deviations of the standard adenine base moiety in both natural and synthetic active site inhibitors, have been shown to be accommodated by various aaRS members. In contrast, our detailed analysis has shown that even subtle changes of the base moiety can dramatically influence ligand affinity for its respective target enzyme. SAR analysis suggests that the presence of a water molecule bridging the N^3-position between adenine and local residues in the active site of class II aaRS, could point to specific recognition of this base in this enzyme class, highlighting the importance of the need to fully understand the pharmacophore of these enzymes for further rational design of inhibitors.

5. Experimental section

5.1. Reagents and chemical analysis

Reagents and solvents were purchased from commercial suppliers (Acros, Sigma-Aldrich, Bachem, Novabiochem) and used as provided, unless indicated otherwise. DMF and THF were of analytical grade and were stored over 4 Å molecular sieves. All other solvents used for reactions were analytical grade and used as provided. Reactions were carried out in oven-dried glassware under a nitrogen atmosphere with stirring at room temperature, unless indicated otherwise. ^{14}C-radiolabeled amino acids and scintillation liquid were purchased from Perkin Elmer.

^{1}H and ^{13}C NMR spectra of the compounds dissolved in $CDCl_3$, CD_3OD, DMSO-d6 or D_2O were recorded on a Bruker UltraShield Avance 300 MHz, 500 MHz or when needed at 600 MHz spectrometer. The chemical shifts are expressed as δ values in parts per million (ppm), using the residual solvent peaks ($CDCl_3$: ^{1}H, 7.26 ppm; ^{13}C, 77.16 ppm; DMSO: ^{1}H, 2.50 ppm; ^{13}C, 39.52 ppm; D_2O: 1H, 4.79 ppm; CD3OD: ^{1}H, 3.31 ppm; ^{13}C, 49.00 ppm) as a reference. Coupling constants are given in Hertz (Hz). The peak patterns are indicated by the following abbreviations: bs = broad singlet, d = doublet, m = multiplet, q = quadruplet, s = singlet and t = triplet. High resolution mass spectra were recorded on a quadrupole time-of-flight mass spectrometer (Q-Tof-2, Micromass, Manchester, UK) equipped with a standard ESI interface; samples were infused in 2- propanol/H2O (1:1) at 3 mL min-1. For TLC, precoated aluminum sheets were used (Merck, Silica gel 60 F254). The spots were visualized by UV light at 254 nm. Chromatography was performed on ICN silica gel 60A 60-200. Final products (acylated sulfamate nucleosides) were purified using a semi-prep PLRP-S 100 Å column (7.5 × 300 mm) connected to a Merck-Hitachi L6200A Intelligent pump. Eluent compositions are expressed as v/v. the characterization of the final compounds by NMR and mass are provided in the supplementary file.

5.2. Chemical synthesis of the intermediates and final compounds

5.2.1. 1H-imidazo[4,5-c]pyridine (**2**)

A mixture of pyridine-3,4-diamine (2 g, 18.3 mmol) and triethyl orthoformate (50 mL) was refluxed for about 3 h at 145 °C. After completion of the reaction monitored by TLC, 2 mL of formic acid was

added and the mixture was refluxed at the same temperature for another 2 h. The solution was evaporated to dryness at reduced pressure, and the residue was dissolved in methanol and stirred at room temperature overnight in presence of charcoal. Following removal of the charcoal by vacuum filtration through celite-545, the filtrate was evaporated to give the title compound **2** as an off-white solid in quantitative yield without further purification. ^{1}H NMR (300 MHz, DMSO-d6) δ 8.97 (d, *J* = 1.1 Hz, 1H), 8.32 (d, *J* = 5.6 Hz, 1H), 7.61 (dd, *J* = 5.6, 1.1 Hz, 1H); ^{13}C NMR (75 MHz, DMSO) δ 144.35, 141.18 (2×C, overlapped), 139.72, 137.73, 109.46. HRMS (ESI): m/z calcd. for $C_6H_6N_3$ $[M+H]^+$: 120.0556; found, 120.0556.

5.2.2. 1H-imidazo[4,5-c]pyridine-5-oxide (**3**)

Compound **2** (2.5 g, 20.83 mmol) was dissolved in a mixture of 60 mL DCM + 30 mL of MeOH and 10.3 g of *m*-CPBA (41.67 mmol) dissolved in methanol was added dropwise at 0 °C. The reaction was stirred at room temperature for 22 h, after which the mixture was concentrated in vacuum. Methanol (30 mL) was added to the residue which was adsorbed on silica. The title compound **3** was isolated via silica gel chromatography using EA/MeOH (65:35) in 80% yield. ^{1}H NMR (300 MHz, DMSO-d6) δ 8.68 (d, J = 1.5 Hz, 1H), 8.39 (s, 1H), 8.07 (dd, J = 6.9, 1.8 Hz, 1H), 7.64 (d, J = 6.9 Hz, 1H). ^{13}C NMR (75 MHz, DMSO) δ 147.96, 137.85, 136.67, 133.51, 128.35, 111.77. HRMS (ESI): m/z calcd. for $C_6H_6N_3O$ $[M+H]^+$: 136.0505; found, 136.0510.

5.2.3. 4-chloro-1H-imidazo[4,5-c]pyridine (**4**)

Compound **2** (255 mg, 1.88 mmol) was dissolved in 10 mL $POCl_3$ and stirred at 110 °C for 3 h until a clear solution was obtained. Excess $POCl_3$ was removed in vacuum and ice was added, followed by adding aqueous ammonia until reaching a pH around 9 and an equivalent amount of MeOH was added. Some precipitate formed and was filtered off, and the filtrate was adsorbed on silica and purified by silica gel chromatography (EA with 5% MeOH) affording **4** in 83% yield. HRMS (ESI): m/z calcd. for $C_6H_5ClN_3$ $[M+H]^+$: 154.0166; found, 154.0171.

5.2.4. 4-chloro-1-(2', 3', 5'-tri-*O*-acetyl-*β*-D-ribofuranosyl)-1H-imidazo[4,5-c]pyridine (**5**)

Compound **4** (231 mg, 1.51 mmol) and 1',2',3',5'-tetra-*O*-acetyl-β-D-ribofuranose (720 mg, 2.26 mmol) were dissolved in 10 mL of dry acetonitrile. A solution of $SnCl_4$ (2.26 mL) was added and the reaction mixture was stirred at room temperature for 16 h. The reaction mixture was diluted with DCM (10 mL) and then poured into 20 mL of an ice cooled saturated sodium bicarbonate solution under stirring and the mixture was filtered by celite. Following separation of the layers, the organic phase was further washed with brine and was co-evaporated with silica, and purified by silica gel chromatography to afford compound **5** in 65% yield. ^{1}H NMR (300 MHz, DMSO-d_6) δ 8.74 (d, *J* = 1.0 Hz, 1H), 8.25 (dd, *J* = 5.7, 1.1 Hz, 1H), 7.87 (dd, *J* = 5.7, 1.1 Hz, 1H), 6.41 (dd, *J* = 6.0, 1.0 Hz, 1H), 5.65 (t, *J* = 6.2 Hz,

1H), 5.45 (dd, *J* = 6.3, 4.8 Hz, 1H), 4.50 – 4.41 (m, 1H), 4.39 (d, *J* = 4.2 Hz, 2H), 2.14 (d, *J* = 1.1 Hz, 3H), 2.08 (d, *J* = 1.1 Hz, 3H), 2.04 (d, *J* = 1.1 Hz, 3H). ^{13}C NMR (75 MHz, DMSO) δ 170.14, 169.60, 169.39, 144.61, 141.80, 141.47, 139.15, 137.52, 107.51, 86.85, 79.94, 72.36, 69.65, 63.03, 20.66, 20.52, 20.32. HRMS (ESI): m/z calcd. for $C_{17}H_{19}ClN_3O_7$ $[M+H]^+$: 412.0906; found, 412.0907.

5.2.5. 4-chloro-1 -*β*-D-ribofruanosyl-1H-imidazo[4,5-c]pyridine (**6**)

Compound **5** (1.635 g, 3.98 mmol) was dissolved in methanolic ammonia (7N, 25 mL) at 0 °C. The reaction was stirred for 4 h while reaching room temperature. The reaction mixture was concentrated in vacuum in presence of silica gel and the main compound was purified by silica gel chromatography using EA/methanol (8:2) in 90% yield. ^{1}H NMR (300 MHz, DMSO-d_6) δ 8.71 (s, 1H), 8.17 (d, *J* = 5.6 Hz, 1H), 7.92 (d, *J* = 5.6 Hz, 1H), 5.94 (d, *J* = 6.3 Hz, 1H), 5.55 (d, *J* = 6.4 Hz, 1H), 5.28 (d, *J* = 4.6 Hz, 1H), 5.21 (t, *J* = 5.1 Hz, 1H), 4.43 – 4.29 (m, 1H), 4.14 (td, *J* = 4.8, 2.9 Hz, 1H), 4.03 (q, *J* = 3.5 Hz, 2H), 3.67 (td, *J* = 5.3, 3.4 Hz, 2H). ^{13}C NMR (75 MHz, DMSO) δ 144.72, 141.23, 141.18, 139.34, 137.63, 107.90, 89.35, 86.25, 74.31, 70.26, 61.22. HRMS (ESI): m/z calcd. for $C_{11}H_{13}ClN_3O_4$ $[M+H]^+$: 286.0589; found, 286.0591.

5.2.6. 3-deazaadenosine (**7**)

Compound **6** (700 mg, 2.46 mmol) was dissolved in 20 mL hydrazine hydrate (98% pure) and the reaction was stirred at 120 °C for 4 h. TLC analysis indicated a new more polar product was formed. The reaction was concentrated in vacuum and the residue was dissolved in 10 mL of water, followed by adding 0.7 mL Raney Ni (50% in water) and stirring for 30 min. The catalyst was filtered off and washed with water (10 mL), the filtrate was evaporated in presence of some silica gel and the title compound was separated by silica gel chromatography in 87% yield. ^{1}H NMR (300 MHz, DMSO-d_6) δ 8.37 (s, 1H), 7.68 (d, *J* = 6.0 Hz, 1H), 7.02 (d, *J* = 6.1 Hz, 1H), 6.63 (s, 2H), 5.80 (d, *J* = 6.2 Hz, 1H), 5.51 (s, 1H), 5.24 (s, 1H), 5.13 (s, 1H), 4.32 (s, 1H), 4.10 (d, *J* = 4.8 Hz, 1H), 4.10 (d, *J* = 4.8 Hz, 1H), 3.98 (d, *J* = 3.4 Hz, 1H), 3.64 (s, 2H). HRMS (ESI): m/z calcd. for $C_{11}H_{15}N_4O_4$ $[M+H]^+$: 267.1087; found, 267.1089.

5.2.7. 3-deaza-2',3'-*O*-isopropylidene-adenosine (**8**)

Compound **7** (300 mg, 1.13 mmol) was dissolved in 20 mL of dry acetone, followed by addition of 2 g p-TSA (12 mmol) and 3 mL 2, 2-dimethoxypropane, and the reaction was stirred at room temperature for 2 h. A precipitate was gradually formed after 2 h but disappeared when the temperature was increased to 50 °C, and stirring was continued for another 2 h. Following completion of the reaction by formation of a less polar product, the reaction was neutralized by adding saturated $NaHCO_3$, and concentrated. The title compound **8** was purified by silica gel chromatography (EA/MeOH 9:1) in 81% yield. ^{1}H NMR (300 MHz, DMSO-d_6) δ 8.73 (s, 1H), 8.19 (d, *J* = 5.6 Hz, 1H), 7.80 (d, *J* = 5.7 Hz, 1H),

7.77 (s, 2H), 6.01 (d, *J* = 7.4 Hz, 1H), 4.60 (dd, *J* = 7.5, 4.7 Hz, 1H), 4.36 (d, *J* = 4.4 Hz, 2H), 4.32 – 4.24 (m, 2H), δ 1.62 (s, 3H), 1.39 (s, 3H). HRMS (ESI): m/z calcd. for $C_{14}H_{19}N_4O_4$ $[M+H]^+$: 307.1401; found, 307.1404.

5.2.8. 3-deaza-2',3'-*O*-isopropylidene-5'-*O*-sulfamate-adenosine (**9**)

Chlorosulfonyl isocyanate (210 mg, 1.5 mmol) was taken into a 10 mL flask and after cooling to 0 °C formic acid (70 mg, 1.5 mmol) was added and the mixture was allowed to stir for 5 min. The resulting solid was dissolved in dry acetonitrile (2 mL) and the solution was cooled to 0 °C and stirred for another 5 h gradually reaching room temperature Compound **8** (100 mg, 0.33 mmol) was dissolved in 10 mL of DMA and cooled to 0 °C, and the obtained sulfamoyl chloride was then added to the stirred solution of compound **8** in DMA and the mixture was stirred overnight. After adding TEA (1 mL) the reaction was stirred for 10 min, followed by adding 2 mL of methanol and further stirring for 15 min. The reaction was concentrated and the residue was partitioned between EA and saturated $NaHCO_3$. The organic layer was further washed with water and brine, and the title compound **9** was purified by silica gel chromatography in 85% yield. ^{1}H NMR (300 MHz, DMSO-d_6) δ 8.29 (s, 1H), 7.70 (d, *J* = 5.8 Hz, 1H), 7.66 (s, 2H), 6.88 (d, *J* = 5.8 Hz, 1H), 6.26 (s, 2H), 6.13 (d, *J* = 3.5 Hz, 1H), 5.21 (dd, *J* = 6.5, 3.5 Hz, 1H), 4.99 (dd, *J* = 6.5, 3.3 Hz, 1H), 4.41 (q, *J* = 4.6 Hz, 1H), 4.15 (dd, *J* = 4.9, 2.0 Hz, 2H), 1.59 (s, 3H), 1.35 (s, 3H). ^{13}C NMR (75 MHz, DMSO) δ 152.63, 141.17, 139.67, 137.40, 126.92, 114.36, 97.21, 90.05, 83.00, 82.10, 80.43, 67.94, 27.01, 25.31.

5.2.9. N^6-[*N*-(*tert*-butoxycarbonyl)glycyl]-3-deaza-2',3'-*O*-isopropylidene-5'-*O*-sulfamate-adenosine (**10**)

Compound **9** (40 mg, 0.1 mmol) and 41 mg N-Boc-L-Gly-OSu were dissolved in 16 mL of dry DMF, followed by adding 30 mg DBU and the reaction was stirred at room temperature for 17 h. The reaction was concentrated and the residue was partitioned between EA and saturated $NaHCO_3$. The organic layer was further washed with water and brine, evaporated at reduced vacuum and was subjected to silica gel chromatography. The title compound **10** was isolated in 60% yield. ^{1}H NMR (300 MHz, DMSO-d_6) δ 8.65 (s, 1H), 8.04 (s, 2H), 7.70 (d, *J* = 6.8 Hz, 1H), 7.25 (d, *J* = 6.8 Hz, 1H), 6.35 (t, *J* = 5.6 Hz, 1H), 6.20 (d, *J* = 3.4 Hz, 1H), 5.22 (dd, *J* = 6.2, 3.4 Hz, 1H), 5.01 (dd, *J* = 6.1, 2.1 Hz, 1H), 4.47 (d, *J* = 2.8 Hz, 1H), 4.10 – 3.98 (m, 2H), 3.92 (dd, *J* = 11.2, 4.2 Hz, 1H), 3.42 (d, *J* = 5.7 Hz, 2H), 1.58 (s, 3H), 1.36 (s, 9H), 1.34 (s, 3H). HRMS (ESI): m/z calcd. for $C_{21}H_{29}N_6O_9S$ $[M-H]^-$: 541.1722; found, 541.1725.

The structure of compound **10** was confirmed by NMR and mass analysis, where in proton NMR the exocyclic 6-amine (purine numbering) traditionally showing a signal at δ 6.0-6.5 ppm had disappeared, while the newly introduced sulfamoyl amine signal of compound **9** remained and slightly shifted from δ 7.7 ppm to δ 7.5 ppm. This undesired reaction at the base moiety is explained by increased nucleophilicity of the heterocyclic amine in removing the 3-nitrogen of the adenine base, establishing the need for base protection.

5.2.10. N^6-benzoyl- 3-deaza-2',3'-*O*-isopropylidene-adenosine (**11**)

Compound **8** (100 mg, 0.33 mmol) was dissolved in 10 mL dry pyridine, followed by adding TMSCl (180 mg, 1.66 mmol) at 0 °C and the reaction was stirred at 0 °C for 4 h. After the starting compound had disappeared on TLC analysis, 300 mg BzCl was added and the mixture was stirred for 3 h at room temperature. The reaction was stopped by adding diluted ammonia (12%, 4 mL) at 0 ºC with stirring. The mixture was extracted with DCM (50 mL) and further washed by brine. The organic layer was concentrated in vacuum and the title compound **11** was purified by silica gel chromatography in 79% yield. ^{1}H NMR (300 MHz, DMSO-d_6) δ 10.73 (s, 1H), 8.56 (s, 1H), 8.23 (d, *J* = 5.6 Hz, 1H), 8.05 (d, *J* = 7.4 Hz, 3H), 7.68 (d, *J* = 5.7 Hz, 1H), 7.66 – 7.50 (m, 2H), 6.23 (d, *J* = 3.4 Hz, 1H), 5.24 (dd, *J* = 6.3, 3.4 Hz, 1H), 5.17 (t, *J* = 5.1 Hz, 1H), 4.98 (dd, *J* = 6.2, 2.6 Hz, 1H), 4.26 (d, *J* = 3.1 Hz, 2H), 1.60 (s, 3H), 1.36 (s, 3H). HRMS (ESI): m/z calcd. for $C_{21}H_{23}N_4O_5$ $[M+H]^+$: 411.1663; found, 411.1660.

5.2.11. N^6-benzoyl- 3-deaza-2',3'-*O*-isopropylidene-5'-*O*-sulfamate-adenosine (**12**)

Compound **11** (100 mg, 0.25 mmol) was dissolved in 10 mL DMA followed by adding sulfamoyl chloride (dissolved in MeCN, 0.4 mmol, prepared separately as described for compound **9**), and the reaction was stirred at room temperature overnight. After adding 0.5 mL of TEA a precipitate was formed, which dissolved after adding 2 mL of MeOH and stirring was continued for another 20 min. The reaction was concentrated in vacuum and the residue was dissolved in EA, washed with saturated $NaHCO_3$, and the title compound **12** was purified by silica gel chromatography in 85% yield (MeOH:EA, 2:98). ^{1}H NMR (300 MHz, DMSO-d_6) δ 10.76 (s, 1H), 8.54 (s, 1H), 8.24 (d, *J* = 5.6 Hz, 1H), 8.06 (d, *J* = 7.5 Hz, 2H), 7.76 – 7.46 (m, 6H), 6.31 (d, *J* = 3.5 Hz, 1H), 5.31 (dd, *J* = 6.4, 3.5 Hz, 1H), 5.04 (dd, *J* = 6.5, 3.2 Hz, 1H), 4.47 (q, *J* = 4.4 Hz, 1H), 4.18 (dd, *J* = 4.7, 2.6 Hz, 2H), 1.61 (s, 3H), 1.37 (s, 3H). ^{13}C NMR (75 MHz, DMSO) δ 165.73, 144.42, 142.65, 140.78, 139.19, 135.13, 134.12, 132.00, 114.43, 105.95, 90.22, 83.00, 82.31, 80.46, 67.97, 27.01, 25.33. HRMS (ESI): m/z calcd. for $C_{21}H_{24}N_5O_7S$ $[M+H]^+$: 489.1391; found, 489.1391.

5.2.12. 5'-*O*-[*N*-(*tert*-butoxycarbonyl-glycyl)]sulfamoyl-N^6-benzoyl-3-deaza-2',3'-*O*-isopropylidene-adenosine (**13a**)

Compound **12** (70 mg, 0.143 mmol) and 58 mg of N-Boc-Gly-OSu were dissolved in 8 mL of dry DMF, followed by adding 33 mg DBU and the reaction was stirred at room temperature overnight. The reaction was concentrated in vacuum and the residue was dissolved in EA, and washed with saturated $NaHCO_3$. The title compound **13a** was purified by silica gel chromatography in 82% yield (EA:hexane, 2:1). 1H NMR (300 MHz, DMSO-d6) δ 10.72 (s, 1H), 8.60 (s, 1H), 8.22 (d, J = 5.5 Hz, 1H), 8.06 (d, J = 7.5 Hz, 2H), 7.96 (s, 1H), 7.77 – 7.46 (m, 3H), 6.33 (s, 1H), 6.23 (d, J = 3.6 Hz, 1H), 5.26 (s, 1H), 5.04 (d, J = 6.5 Hz, 1H), 4.44 (s, 1H), 4.12 – 3.87 (m, 2H), 1.60 (s, 3H), 1.35 (d, J = 2.4 Hz, 12H). HRMS (ESI): m/z calcd. for $C_{28}H_{33}N_6O_{11}S$ $[M-H]^-$: 645.1984; found, 645.1984.

5.2.13. 5'-*O*-[*N*-(*tert*-butoxycarbonyl-4-benzyloxy-L-tyrosyl)]sulfamoyl-N^6-benzoyl-3-deaza-2',3'-*O*-isopropylidene-adenosine (**13b**)

This compound was synthesized in analogy to **13a**. Yield: 68%. HRMS (ESI): m/z calcd. for $C_{42}H_{45}N_6O_{11}S$ $[M-H]^-$: 841.2872; found, 841.2867.

5.2.14. 5'-*O*-[*N*-(*tert*-butoxycarbonyl-*O*-benzyl-L-seryl)]sulfamoyl-N^6-benzoyl-3-deaza-2',3'-*O*-isopropylidene-adenosine (**13c**)

This compound was synthesized in analogy to **13a**. Yield: 71%. HRMS (ESI): m/z calcd. for $C_{36}H_{41}N_6O_{11}S$ $[M+H]^+$: 767.2705; found, 767.2722.

5.2.15. 5'-*O*-[*N*-(*tert*-butoxycarbonyl-*O*-*tert*-butyl-L-aspartyl)]sulfamoyl-N^6-benzoyl-3-deaza-2',3'-*O*-isopropylidene-adenosine (**13d**)

This compound was synthesized in analogy to **13a**. Yield: 85%. HRMS (ESI): m/z calcd. for $C_{34}H_{43}N_6O_{12}S$ $[M-H]^-$: 759.2665; found, 759.2673.

5.2.16. 5'-*O*-[*N*-(*tert*-butoxycarbonyl-L-leucyl)]sulfamoyl-N^6-benzoyl-3-deaza-2',3'-*O*-isopropylidene-adenosine (**13e**)

This compound was synthesized in analogy to **13a**. Yield: 87%. HRMS (ESI): m/z calcd. for $C_{32}H_{41}N_6O_{10}S$ $[M-H]^-$: 701.2610; found, 701.2598.

5.2.17. 5'-*O*-[*N*-(*tert*-butoxycarbonyl-L-isoleucyl)]sulfamoyl-N^6-benzoyl-3-deaza-2',3'-*O*-isopropylidene-adenosine (**13f**)

This compound was synthesized in analogy to **13a**. Yield: 89%. HRMS (ESI): m/z calcd. for $C_{32}H_{41}N_6O_{10}S$ $[M-H]^-$: 701.2610; found, 701.2612.

5.2.18. 5'-*O*-[*N*-(*tert*-butoxycarbonyl-glycyl)]sulfamoyl-3-deaza-2',3'-*O*-isopropylidene-adenosine (**14a**)

A solution of compound **13a** in methanol (10 mL) was treated with 2 drops of 30% sodium methoxide in methanol and the solution was refluxed for 2.5 h when according to TLC the reaction was completed. The mixture was concentrated and adsorbed on silica at reduced vacuum. The title compound **14a** was purified by silica gel chromatography (MeOH:EA, 18:82) in 90% yield. ^{1}H NMR (300 MHz, DMSO-d_6) δ 8.50 (s, 1H), 7.70 (d, *J* = 6.2 Hz, 1H), 7.19 – 7.01 (m, 3H), 6.33 (s, 0H), 6.13 (d, *J* = 3.5 Hz, 1H), 5.19 (d, *J* = 4.1 Hz, 1H), 5.05 – 4.93 (m, 1H), 4.42 (s, 1H), 4.07 – 3.96 (m, 2H), 3.91 (dd, *J* = 11.2, 4.5 Hz, 1H), 1.58 (s, 3H), 1.35 (d, 12H). ^{13}C NMR (75 MHz, DMSO) δ 173.74,

155.59, 151.04, 141.03, 138.22, 126.73, 113.67, 98.10, 90.89, 83.35, 83.21, 81.24, 77.62, 66.79, 45.83, 45.76, 28.39, 27.04, 25.28. HRMS (ESI): m/z calcd. for $C_{21}H_{29}N_6O_9S$ $[M-H]^-$: 541.1722; found, 541.1725.

5.2.19. 5'-*O*-[*N*-(*tert*-butoxycarbonyl-4-benzyloxy-L-tyrosyl)]sulfamoyl-3-deaza-2',3'-*O*-isopropylidene-adenosine (**14b**)

This compound was synthesized in analogy to **14a**. Yield: 91%. HRMS (ESI): m/z calcd. for $C_{35}H_{43}N_6O_{10}S$ $[M+H]^+$: 739.2756; found, 739.2774.

5.2.20. 5'-*O*-[*N*-(*tert*-butoxycarbonyl-*O*-benzyl-L-seryl)]sulfamoyl-3-deaza-2',3'-*O*-isopropylidene-adenosine (**14c**)

This compound was synthesized in analogy to **14a**. Yield: 89%. HRMS (ESI): m/z calcd. for $C_{29}H_{39}N_6O_{10}S$ $[M+H]^+$: 663.2443; found, 663.2452.

5.2.21. 5'-*O*-[*N*-(*tert*-butoxycarbonyl-*O*-*tert*-butyl-L-aspartyl)]sulfamoyl-3-deaza-2',3'-*O*-isopropylidene-adenosine (**14d**)

This compound was synthesized in analogy to **14a**. Yield: 89%. HRMS (ESI): m/z calcd. for $C_{27}H_{39}N_6O_{11}S$ $[M-H]^-$: 655.2403; found, 655.2396.

5.2.22. 5'-*O*-[*N*-(*tert*-butoxycarbonyl-L-leucyl)]sulfamoyl-3-deaza-2',3'-*O*-isopropylidene-adenosine (**14e**)

This compound was synthesized in analogy to **14a**. Yield: 93%. HRMS (ESI): m/z calcd. for $C_{25}H_{37}N_6O_9S$ $[M-H]^-$: 597.2348; found, 597.2347.

5.2.23. 5'-*O*-[*N*-(*tert*-butoxycarbonyl-L-isoleucyl)]sulfamoyl-3-deaza-2',3'-*O*-isopropylidene-adenosine (**14f**)

This compound was synthesized in analogy to **14a**. Yield: 94%. HRMS (ESI): m/z calcd. for $C_{25}H_{37}N_6O_9S$ $[M-H]^-$: 597.2348; found, 597.2349.

5.2.24. 5'-*O*-(*N*-glycyl)sulfamoyl-3-deaza-adenosine (15a)

Compound **14a** (60 mg, 0.11 mmol) was dissolved in a solvent mixture of TFA and H_2O (7 mL, 5:2 v/v) and the reaction mixture was stirred for 40 min. After reaction, the volatiles were evaporated under reduced pressure, followed by co-evaporation with EtOH, and once more with EtOH + 1 mL Et_3N to neutralize any remaining acid. The title compound **15a** was obtained by RP-HPLC as a white solid in 60% yield. ^{1}H NMR (300 MHz, deuterium oxide) δ 8.38 (s, 1H), 7.55 (d, *J* = 7.0 Hz, 1H), 7.14 (d, *J* =

7.1 Hz, 1H), 5.95 (d, *J* = 5.8 Hz, 1H), 4.55 – 4.29 (m, 6H), 3.61 (s, 1H), 3.11 (q, *J* = 7.3 Hz, 1H), 1.19 (t, *J* = 7.3 Hz, 1.5H) (δ 3.11 and 1.19 belonging to triethylamine). ^{13}C NMR (75 MHz, D_2O) δ 172.48, 148.16, 142.46, 139.03, 130.30, 125.84, 99.29, 88.92, 82.59, 73.96, 69.73, 67.94, 46.34, 42.44, 7.88 (δ 46.34 and 7.88 belonging to triethylamine). HRMS (ESI): m/z calcd. for $C_{13}H_{19}N_6O_7S$ $[M+H]^+$: 403.1030; found, 403.1032.

5.2.25. 5'-*O*-(*N*-L-tyrosyl)sulfamoyl-3-deaza-adenosine (**15b**)

To a solution of compound **14b** (130 mg, 0.176 mmol) in methanol (10 mL) was added 69 mg Pd/C under argon, after which the argon was changed to hydrogen and the mixture was stirred at room temperature overnight. TLC analysis indicated the reaction to be completed, and the Pd/C was filtered and the filtrate was concentrated. The residue was adsorbed on silica and was purified by chromatography (MeOH/EA, 1:9) in 57% yield. Mass for the intermediate: HRMS (ESI): m/z calcd for $C_{28}H_{37}N_6O_{10}S$ $[M+H]^+$: 649.2286; found, 649.2282. The obtained compound (65 mg, 0.1 mmol) was dissolved in a solvent mixture of TFA and H_2O (7 mL, 5:2 v/v) and the reaction mixture was stirred for 30 min. The volatiles were evaporated under reduced pressure followed by co-evaporation with EtOH, and once more with EtOH + 1 mL Et_3N to neutralize any remaining acid. The title compound **15b** was obtained by RP-HPLC as a white solid in 42% yield. ^{1}H NMR (300 MHz, deuterium oxide) δ 8.21 (s, 1H), 7.65 (d, *J* = 6.2 Hz, 1H), 7.04 – 6.89 (m, 3H), 6.62 (d, *J* = 8.3 Hz, 2H), 5.91 (d, *J* = 6.0 Hz, 1H), 4.49 (t, *J* = 5.3 Hz, 1H), 4.33 (s, 2H), 4.20 (d, *J* = 6.2 Hz, 1H), 3.75 (t, *J* = 6.4 Hz, 1H), 3.11 (q, *J* = 7.4 Hz, 2H,), 2.96 – 2.76 (m, 2H), 1.19 (t, *J* = 7.3 Hz, 3H) (δ 3.11 and 1.19 belonging to triethylamine). ^{13}C NMR (75 MHz, D_2O) δ 176.48, 154.42, 148.24, 140.91, 139.12, 138.08, 130.38, 126.36, 122.29, 115.14, 98.90, 88.59, 82.24, 73.54, 69.76, 68.02, 56.68, 46.36, 36.49, 7.90 (δ 46.36 and 7.90 belonging to triethylamine). HRMS (ESI): m/z calcd. for $C_{20}H_{25}N_6O_8S$ $[M+H]^+$: 509.1449; found, 509.1450.

5.2.26. 5'-*O*-(*N*-L-seryl)sulfamoyl-3-deaza-adenosine (**15c**)

A solution of compound **14c** (93 mg, 0.15 mmol) in methanol (10 mL) was processed in analogy with **15b**. Purification by silica gel chromatography (MeOH/EA, 1:9) afforded the debenzylated intermediate in 69% yield (54 mg, 0.09 mmol) which was processed in analogy with **15a**. The title compound **15c** was separated by RP-HPLC as a white solid in 54% yield. ^{1}H NMR (300 MHz, deuterium oxide) δ 8.27 (s, 1H), 7.47 (d, *J* = 6.8 Hz, 1H), 6.98 (d, *J* = 6.8 Hz, 1H), 5.86 (d, *J* = 5.9 Hz, 1H), 4.45 (dd, *J* = 5.9, 4.9 Hz, 1H), 4.33 (dt, *J* = 9.7, 3.5 Hz, 4H), 3.88 (m, 3H), 3.09 (q, *J* = 7.3 Hz, 4H), 1.17 (t, *J* = 7.3 Hz, 6H) (δ 3.09 and 1.17 belonging to triethylamine). ^{13}C NMR (75 MHz, D_2O) δ 173.02, 148.24, 142.11, 138.52, 131.66, 125.50, 117.95, 114.08, 98.97, 88.86, 82.50, 73.98, 69.73, 68.09, 60.06, 56.71, 46.32, 7.87 (δ 46.32 and 7.87 belonging to triethylamine). HRMS (ESI): m/z calcd for $C_{14}H_{19}N_6O_8S$ $[M-H]^-$: 431.0990; found, 431.0990. Mass for the intermediate: HRMS (ESI): m/z calcd. for $C_{22}H_{33}N_6O_{10}S$ $[M+H]^+$: 573.1973; found, 573.1982.

5.2.27. 5'-*O*-(*N*-L-aspartyl)sulfamoyl-3-deaza-adenosine (**15d**)

Compound **14d** (90 mg, 0.137 mmol) was processed in analogy with **15a**. The title compound **15d** was separated by RP-HPLC as a white solid in 53% yield. ^{1}H NMR (300 MHz, deuterium oxide) δ 8.31 (d, *J* = 1.2 Hz, 1H), 7.46 (dd, *J* = 7.1, 1.2 Hz, 1H), 7.04 (dd, *J* = 7.1, 1.2 Hz, 1H), 5.86 (dd, *J* = 6.2, 1.2 Hz, 1H), 4.46 – 4.26 (m, 5H), 3.92 (ddd, *J* = 6.1, 4.7, 1.2 Hz, 1H), 3.10 (q, *J* = 7.4, 3H), 2.71 (td, *J* = 4.7, 1.2 Hz, 2H), 1.18 (td, *J* = 7.3, 1.2 Hz, 4H) (δ 3.10 and 1.18 belonging to triethylamine). ^{13}C NMR (75 MHz, D_2O) δ 176.56, 174.79, 147.84, 142.62, 138.77, 129.88, 125.57, 99.17, 88.86, 82.84, 74.05, 69.81, 68.12, 52.61, 46.34, 36.26, 7.89 (δ 46.34 and 7.89 belonging to triethylamine). HRMS (ESI): m/z calcd. for $C_{15}H_{19}N_6O_9S$ $[M-H]^-$: 459.0940; found, 459.0945.

5.2.28. 5'-*O*-(*N*-L-leucyl)sulfamoyl-3-deaza-adenosine (**15e**)

Compound **14e** (60 mg, 0.1 mmol) was deprotected analogously to **14d**. The title compound **15e** was separated by RP-HPLC as a white solid in 70% yield. ^{1}H NMR (300 MHz, deuterium oxide) δ 8.20 (s, 1H), 7.55 (d, *J* = 6.2 Hz, 1H), 6.91 (d, *J* = 6.2 Hz, 1H), 5.85 (d, *J* = 6.0 Hz, 1H), 4.50 – 4.26 (m, 5H), 3.65 (d, *J* = 6.6 Hz, 1H), 1.69 – 1.36 (m, 3H), 0.73 (d, 6H). ^{13}C NMR (75 MHz, D_2O) δ 176.38, 150.14, 141.05, 137.95, 137.80, 125.99, 98.86, 88.60, 82.37, 73.60, 69.79, 67.98, 53.91, 40.02, 23.65, 21.44, 20.54. HRMS (ESI): m/z calcd. for $C_{17}H_{25}N_6O_7S$ $[M-H]^-$: 457.1510; found, 457.1507.

5.2.29. 5'-*O*-(*N*-L-isoleucyl)sulfamoyl-3-deaza-adenosine (**15f**)

Compound **14f** (60 mg, 0.1 mmol) was deprotected analogously to **14d**. The title compound **15f** was separated by RP-HPLC as a white solid in 75% yield. ^{1}H NMR (300 MHz, deuterium oxide) δ 8.20 (s, 1H), 6.91 (d, *J* = 6.2 Hz, 1H), 5.85 (d, *J* = 6.1 Hz, 1H), 4.56 – 4.18 (m, 5H), 3.59 (d, *J* = 4.1 Hz, 1H), 1.94 – 1.75 (m, 1H), 1.29 (ddd, *J* = 12.6, 7.5, 4.8 Hz, 1H), 1.04 (ddd, *J* = 13.4, 9.4, 7.1 Hz, 1H), 0.82 (d, *J* = 7.0 Hz, 3H), 0.67 (t, *J* = 7.4 Hz, 3H). ^{13}C NMR (75 MHz, D_2O) δ 175.12, 150.25, 140.99, 138.14, 137.97, 126.03, 99.66, 98.85, 88.54, 82.34, 73.55, 69.77, 67.98, 59.81, 36.15, 23.73, 14.13, 10.51. HRMS (ESI): m/z calcd. for $C_{17}H_{25}N_6O_7S$ $[M-H]^-$: 457.1510; found, 457.1505.

5.3. *E. coli* S30 cell whole extracts inhibition assays

10 µL of an *E. coli* K-12 BW28357 strain glycerol stock was used to inoculate 5 mL of LB-medium and shaken at 180 rpm and 37 °C, overnight. 50 µL of this pre-culture was used to inoculate 50 mL LB-medium and grow the culture until the absorbance at 600 nm of 0.5. Cells where then centrifuged at 3000 g for 10 min and the media discarded. The cell pellet was resuspended in 40 mL buffer containing 20 mM Tris.HCl, 10 mM $MgCl_2$, 100 mM KCl, pH 8.0. The cell suspension was centrifuged again at 3000 g. This procedure was repeated twice. The pellet was the resuspended in 1 mL of the

same buffer containing in addition 1 mM DTT and kept at 0 °C. Subsequently, the cells were sonicated for 10 s and left at 0 °C for 10 min. This procedure was repeated 5-8 times. The lysate was centrifuged at 15,000 g for 30 min at +4 °C using a bench-top centrifuge.

For the tRNA aminoacylation a 20 µl reaction was prepared. First, 1 µl of the inhibitor (at a stock concentration of 50 µM) or water was added to 3 µl of the *E. coli* extract and incubated for 5 min. Next, 16 µl of the following aminoacylation mixture was added: Tris.HCl (30 mM, pH 8.0), DTT (1 mM), *E. coli* tRNA (5 g/L), ATP (3 mM), KCl (30 mM), $MgCl_2$ (8 mM), and the specified ^{14}C-radiolabeled amino acid (40 µM, see supplementary file). The reaction products were precipitated in cold 10% TCA on Whatman 3 MM paper, 5 min after the aminoacylation mixture was added. The aminoacylation reaction was carried out at room temperature. After thorough washing with cold 10% TCA, the papers were washed twice with acetone and dried on a heating plate. Following the addition of scintillation liquid (12 mL), the amount of radionuclide incorporation was determined using a Tri-card 2300 TR liquid scintillation counter.

5.4. Cloning, expression and purification of *E. coli* aminoacyl-tRNA synthetases

Sequences encoding for aspRS, ileRS, leuRS, glyRS, serRS and tyrRS were amplified from genomic DNA isolated from the *E. coli* B strain derivative *E. coli* BL21 (DE3). Sequences for the forward and reverse primer can be found in the supplementary file. The coding sequences for aspRS, ileRS, leuRS and tyrRS were cloned into pETRUK (an in-house sumo fusion plasmid containing a pI modified sumo sequence). SerRS and glyRS were cloned into pETHSUK, a derivative of pETHSUL containing an additional KpnI cleavage site in the MCS. In the case of glyRS, which is a hetero-tetramer composed of two different monomers, the encoding genes (glyQ and glyS) were cloned separately into the pETHSUK vector. For all constructs, except aspRS, cloning was performed such that upon expression and purification the final cleaved product contained no non-native amino acids. In the specific case of aspRS, initial trials showed that the sumo hydrolase failed to cleave the sumo-aspRS fusion at the start methionine therefore an additional glycine spacer was placed between the terminal sumo residue and the first residue of aspRS. Overexpression of all constructs was carried out in the *E. coli* Rosetta 2 (DE3) pLysS strain. Further, culturing, cell harvesting and isolation of proteins is detailed in the supplementary section.

5.5. tRNA purification

BL21 (DE3) *E.coli* cells were grown overnight in 50 mL LB media at 30°C. 25 mL of the preculture was transferred to 2L LB media and grown at 37°C until an absorbance at 600nm of 0.6 was reached at which point the cells were harvested by centrifugation at 7000g at 4°C. Total RNA was extracted using guanidinium thiocyanate-phenol-chloroform method [43]. The RNA was precipitated using 3 volumes of isopropanol and stored at -20°C until further workup. The precipitated total RNA was resuspended using 200 mM TRIS pH 9 and incubate for 1 h at 37 °C to deacylate all tRNA prior to loading onto a two 5 mL Hitrap Q HP columns (GE Lifesciences). The column was washed with 5 CV of buffer A (20 mM TRIS pH 7.5, 10 mM $MgCl_2$, 300 mM NaCl) followed by elution of the RNA

using a gradient from 0-55 % Buffer B (20 mM TRIS pH 7.5, 10 mM $MgCl_2$, 1 M NaCl) over 20 CV. The tRNA containing fractions were combined and the tRNA was precipitated using 3 volumes of isopropanol and stored at -20°C. Prior to use, the tRNA was resuspended in assay buffer.

5.6. Purified aaRS inhibition assays

To examine the inhibitory effect of the aaSA and aaS3DA compounds we performed a radiolabel transfer assay using purified *E. coli* aaRS [31]. Briefly, either 50 nM ileRS, 0.5 nM tyrRS, 2.5 nM leuRS, 2 nM aspRS, 2 nM serRS or 2 nM glyRS in 20 mM Tris, 100 mM KCl, 10 mM $MgCl_2$, 5 mM β-mercaptoethanol, pH 7.5 was pre-incubated with the compound, at different concentrations, at 37°C in the presence of 50 µM of the appropriate ^{14}C-labeled amino acid, 2 mg/ml tRNA and 0.5 mg/ml inorganic pyrophosphatase. After 10 min, pre-warmed ATP was added to the mixture at a final concentration of 500 µM. The reaction was quenched by addition of 0.2 M sodium acetate pH 4, 0.1% N-lauroylsarcosine and 5 mM unlabeled amino acid (2 mM for tyrosine). 20 µL was spotted on 3MM Whatmann paper, precipitated using cold 10% TCA, washed twice with 10 % TCA and once with acetone and dried. Addition of scintillation liquid was followed by measurement of the radio activity using scintillation counter. The linear zone of enzyme activity was determined for each aaRS. The quench time point was picked within this zone and with approximately 50% of total RNA aminoacylation. Copeland pointed out [44] that when the K_i^{app} of the compound approaches or is lower than the used enzyme concentration the Michaelis-Menten equation is no longer valid. Therefore, the K_i^{app} was determined using the Greco-Hakala equation:

$$Fractional\ activity\ (\%) = \frac{E_0 - I_0 - K_i^{app} + \sqrt{(E_0 - I_0 - K_i^{app})^2 + 4E_0K_i^{app}}}{2E_0}$$

The fractional activity is determined in the presence of a range of inhibitors (Io). The K_i^{app} and E_0 are the parameters of the equation.

5.7. MIC determination

All compounds were screened for their in vitro antibacterial activity against representative Gram-positive, Gram-negative strains or yeast, by means of standard twofold serial dilution method using LB media. The 50% minimum inhibitory concentration (MIC_{50}) is defined as the minimum concentration of the compound required to give 50% inhibition of bacterial growth after incubation at 37 □ for 18-24 h.

5.8. Quantum calculations

Calculations of the electrostatic potential were done by Gamess program (version released on Aug 18, 2016), and graphics produced by Molden version 5.7. Structures were first energy optimized at radial distribution functions RHF/6-31G** basis set, five basic colours used at the potential contour values: red -0.1, yellow -0.05, green 0.000, light blue 0.05, blue 0.1 (Left: 9-methyladenine, right: 3-deaza-9-methyladenine). To simulate nucleosides, the bases were capped with a methyl group at N^9.

5.9. Bioinformatic analysis

X-ray crystallographic structures of various *E. coli* aaRS were identified in the Protein Databank (PDB). For the enzymes where no coordinates were available, structures were downloaded from the *E. coli* template based protein structure prediction dataset [45]. The coordinates were split into two groups based on the aaRS class type. The structures in each group were aligned by structural superposition of the catalytic core using UCSF chimera [46]. Homologous aaRS sequences, identified in the genome of the methicillin resistant *Staphylococcus aureus* subsp. aureus HO 5096 0412, were added to the two structure-based alignments using the MAFFT online server [47]. In case of the class I alignment no homologue of glnRS was identified in the *S. aureus* genome as this species utilizes the Glu-$tRNA^{gln}$ amidotransferase to generate the correct aminoacylated tRNA. The resultant alignments we further manually modified using Jalview [48]. Also for the class I alignment the leuRS specific insert, that is uniquely found between the end of the core catalytic domain and the start of the KMSKS loop in this aaRS, was removed. Sequence logos of identified core regions were generated using the WebLogo 3 server [49].

Supplementary data

Supplementary Data related to this article can be found on online.

Acknowledgement

The authors thank the China Scholarship Council for providing scholarships to Baole Zhang and Luping Pang, the Belgian FWO for providing a SB Fellowship of the Research Foundation - Flanders to Steff De Graef and KU Leuven for financial support. Mass spectrometry was made possible by the support of the Hercules Foundation of the Flemish Government [20100225E7]. We are also indebted to Luc Baudemprez for help with NMR spectra measurement and Jef Rozenski for providing MS analysis. (Manesh mentioned to me that maybe his grand should be mentioned as well)

Funding

This work was supported by the Research Fund Flanders [Fonds voor Wetenschappelijk Onderzoek, G077814N to S.S. and A.V., G0A4616N to S.W. and A.V., 12A3916N to B.G., G077814N to M.N.

1S53516N to S. D. G.]; and the KU Leuven Research Fund [3M14022 to S.W and A.V.]; and the Chinese Scholarship Council [to Z.B. and LP].

Conflict interest

No conflicts of interest are declared.

References

[1] C.D. Mathers, T. Boerma, D. Ma Fat, Global and regional causes of death, Br. Med. Bull., 92 (2009) 7-32.
[2] C.D. Mathers, D.M. Fat, M. Inoue, C. Rao, A.D. Lopez, Counting the dead and what they died from: an assessment of the global status of cause of death data, Bull. W. H. O., 83 (2005) 171-177.
[3] B. Papp, V. Lazar, Antibiotics: New recipe for targeting resistance, Nat. Chem. Biol., 12 (2016) 891-892.
[4] J. O'Neill, Antimicrobial resistance: Tackling a crisis for the health and wealth of nations, (2014) 1-20.
[5] P. Fang, M. Guo, Evolutionary Limitation and Opportunities for Developing tRNA Synthetase Inhibitors with 5-Binding-Mode Classification, Life, 5 (2015) 1703-1725.
[6] C.R. Woese, G.J. Olsen, M. Ibba, D. Söll, Aminoacyl-tRNA Synthetases, the Genetic Code, and the Evolutionary Process, Microbiol. Mol. Biol. Rev., 64 (2000) 202-236.
[7] M. Ibba, D. Schimmell, Aminoacyl-tRNA synthesis, Annu. Rev. Biochem., 69 (2000) 617-650.
[8] I. Hanukoglu, Proteopedia: Rossmann fold: A beta-alpha-beta fold at dinucleotide binding sites, Biochem. Mol. Biol. Educ., 43 (2015) 206-209.
[9] G. Eriani, M. Delarue, O. Poch, J. Gangloff, D. Moras, Partition of tRNA synthetases into two classes based on mutually exclusive sets of sequence motifs, Nature, 347 (1990) 203-206.
[10] J.J. Perona, A. Hadd, Structural Diversity and Protein Engineering of the Aminoacyl-tRNA Synthetases, Biochemistry, 51 (2012) 8705-8729.
[11] J. Pohlmann, H. Brotz-Oesterhelt, New aminoacyl-tRNA synthetase inhibitors as antibacterial agents, Curr. Drug Targets: Infect. Disord., 4 (2004) 261-272.
[12] L.L. Silver, Challenges of Antibacterial Discovery, Clin. Microbiol. Rev., 24 (2011) 71-109.
[13] D.J. Hetem, M.J. Bonten, Clinical relevance of mupirocin resistance in Staphylococcus aureus, J. Hosp. Inf., 85 (2013) 249-256.
[14] C.P. Randall, D. Rasina, A. Jirgensons, A.J. O'Neill, Targeting Multiple Aminoacyl-tRNA Synthetases Overcomes the Resistance Liabilities Associated with Antibacterial Inhibitors Acting on a Single Such Enzyme, Antimicrob. Agents Chemother., 60 (2016) 6359-6361.
[15] S.C. Sukuru, T. Crepin, Y. Milev, L.C. Marsh, J.B. Hill, R.J. Anderson, J.C. Morris, A. Rohatgi, G. O'Mahony, M. Grøtli, F. Danel, M.G. Page, M. Härtlein, S. Cusack, M.A. Kron, L.A. Kuhn, Discovering New Classes of Brugia malayi Asparaginyl-tRNA Synthetase Inhibitors and Relating Specificity to Conformational Change, J. Comput.-Aided Mol. Des., 20 (2006) 159-178.
[16] S. Bernier, D.Y. Dubois, M. Therrien, J. Lapointe, R. Chênevert, Synthesis of Glutaminyl Adenylate Analogues that are inhibitors of glutaminyl-tRNA synthetase, Bioorg. Med. Chem. Lett., 10 (2000) 2441-2444.
[17] P. Brown, C.M. Richardson, L.M. Mensah, P.J. O'Hanlon, N.F. Osborne, A.J. Pope, G. Walker, Molecular recognition of tyrosinyl adenylate analogues by prokaryotic tyrosyl tRNA synthetases, Bioorg. Med. Chem., 7 (1999) 2473-2485.

[18] A.K. Forrest, R.L. Jarvest, L.M. Mensah, P.J. O'Hanlon, A.J. Pope, R.J. Sheppard, Aminoalkyl adenylate and aminoacyl sulfamate intermediate analogues differing greatly in affinity for their cognate *Staphylococcus aureus* aminoacyl tRNA synthetases, Bioorg. Med. Chem. Lett., 10 (2000) 1871-1874.
[19] J. Lee, S.U. Kang, M.K. Kang, M.W. Chun, Y.J. Jo, J.H. Kkwak, S. Kim, Methionyl adenylate analogues as inhibitors of methionyl-tRNA synthetase, Bioorg. Med. Chem. Lett., 9 (1999) 1365-1370.
[20] J. Lee, S.U. Kang, S.Y. Kim, S.E. Kim, Y.J. Jo, S. Kim, Vanilloid and isovanilloid analogues as inhibitors of methionyl-tRNA and isoleucyl-tRNA synthetases, Bioorg. Med. Chem. Lett., 11 (2001) 965-968.
[21] J. Lee, S.U. Kang, S.Y. Kim, S.E. Kim, M.K. Kang, Y.J. Jo, S. Kim, Ester and hydroxamate analogues of methionyl and isoleucyl adenylates as inhibitors of methionyl-tRNA and isoleucyl-tRNA synthetases, Bioorg. Med. Chem. Lett., 11 (2001) 961-964.
[22] J.E. Hodgson, S.P. Curnock, K.G. Dyke, R. Morris, D.R. Sylvester, M.S. Gross, Molecular characterization of the gene encoding high-level mupirocin resistance in Staphylococcus aureus J2870, Antimicrob. Agents Chemother., 38 (1994) 1205-1208.
[23] M.J.B. Brown, L.M. Mensah, M.L. Doyle, N.J.P. Broom, N. Osbourne, A.K. Forrest, C.M. Richardson, P.J. O'Hanlon, A.J. Pope, Rational design of femtomolar inhibitors of isoleucyl tRNA synthetase from a binding model for pseudomonic acid-A, Biochemistry, 39 (2000) 6003-6011.
[24] D. Heacock, C.J. Forsyth, K. Shiba, K. Musier-Forsyth, Synthesis and aminoacyl-tRNA synthetase inhibitory activity of prolyl adenylate analogs, Bioorg. Chem., 24 (1996) 273-289.
[25] H. Ueda, Y. Shoku, N. Hayashi, J.-i. Mitsunaga, Y. In, M. Doi, M. Inoue, T. Ishida, X-ray crystallographic conformational study of 5′-O-[N-(l-alanyl)-sulfamoyl]adenosine, a substrate analogue for alanyl-tRNA synthetase, Biochim. Biophys. Acta, Protein Struct. Mol. Enzymol., 1080 (1991) 126-134.
[26] J. Lee, S.E. Kim, J.Y. Lee, S.Y. Kim, S.U. Kang, S.H. Seo, M.W. Chun, T. Kang, S.Y. Choi, H.O. Kim, *N*-Alkoxysulfamide, *N*-hydroxysulfamide, and sulfamate analogues of methionyl and isoleucyl adenylates as inhibitors of methionyl-tRNA and isoleucyl-tRNA synthetases, Bioorg. Med. Chem. Lett., 13 (2003) 1087-1092.
[27] B. Gadakh, S. Smaers, J. Rozenski, M. Froeyen, A. Van Aerschot, 5′-(N-aminoacyl)-sulfonamido-5′-deoxyadenosine: Attempts for a stable alternative for aminoacyl-sulfamoyl adenosines as aaRS inhibitors, Eur. J. Med. Chem., 93 (2015) 227-236.
[28] I.N. Redwan, T. Ljungdahl, M. Grøtli, Investigation, optimization and synthesis of sulfamoyloxy-linked aminoacyl-AMP analogues, Tetrahedron, 68 (2012) 1507-1514.
[29] P. Van de Vijver, G.H. Vondenhoff, T.S. Kazakov, E. Semenova, K. Kuznedelov, A. Metlitskaya, A. Van Aerschot, K. Severinov, Synthetic microcin C analogs targeting different aminoacyl-tRNA synthetases, J. Bacteriol., 191 (2009) 6273-6280.
[30] B.P. Duckworth, T.W. Geders, D. Tiwari, H.I. Boshoff, P.A. Sibbald, C.E. Barry, 3rd, D. Schnappinger, B.C. Finzel, C.C. Aldrich, Bisubstrate adenylation inhibitors of biotin protein ligase from Mycobacterium tuberculosis, Chem. Biol., 18 (2011) 1432-1441.
[31] B. Gadakh, G. Vondenhoff, E. Lescrinier, J. Rozenski, M. Froeyen, A. Van Aerschot, Base substituted 5′-O-(N-isoleucyl)sulfamoyl nucleoside analogues as potential antibacterial agents, Bioorg. Med. Chem., 22 (2014) 2875-2886.
[32] F. Seela, H. Rosemeyer, S. Fischer, Synthesis of 3-Deaza-2′-deoxyadenosine and 3-Deaza-2′,3′-dideoxyadenosine: Glycosylation of the 4-Chloroimidazo[4,5-c]pyridinyl Anion, Helv. Chim. Acta, 73 (1990) 1602-1611.
[33] T.A. Devlin, D.J. Jebaratnam, An Improved Procedure for the Synthesis of 1,3-Dideazaadenosine, Synth. Commun., 25 (1995) 711-718.
[34] O. Bande, P. Herdewijn, A Convenient Route for the Synthesis of 3-Deazaspongosine, Eur. J. Org. Chem., 2014 (2014) 231-236.

[35] C. Shi, D. Tiwari, D.J. Wilson, C.L. Seiler, D. Schnappinger, C.C. Aldrich, Bisubstrate Inhibitors of Biotin Protein Ligase in Mycobacterium tuberculosis Resistant to Cyclonucleoside Formation, ACS Med. Chem. Lett., 4 (2013) 1213-1217.
[36] J. Ombouma, D. Vullo, P. Dumy, C.T. Supuran, J.-Y. Winum, Carbonic Anhydrase Glycoinhibitors belonging to the Aminoxysulfonamide Series, ACS Med. Chem. Lett., 6 (2015) 819-821.
[37] P. Van de Vijver, T. Ostrowski, B. Sproat, J. Goebels, O. Rutgeerts, A. Van Aerschot, M. Waer, P. Herdewijn, Aminoacyl-tRNA synthetase inhibitors as potent and synergistic immunosuppressants, J. Med. Chem., 51 (2008) 3020-3029.
[38] L. Zhang, A. Peritz, E. Meggers, A simple glycol nucleic acid, J. Am. Chem. Soc., 127 (2005) 4174-4175.
[39] J.F. Gerster, K.J. Lindstrom, R.L. Miller, M.A. Tomai, W. Birmachu, S.N. Bomersine, S.J. Gibson, L.M. Imbertson, J.R. Jacobson, R.T. Knafla, P.V. Maye, N. Nikolaides, F.Y. Oneyemi, G.J. Parkhurst, S.E. Pecore, M.J. Reiter, L.S. Scribner, T.L. Testerman, N.J. Thompson, T.L. Wagner, C.E. Weeks, J.-D. Andre, D. Lagain, Y. Bastard, M. Lupu, Synthesis and Structure−Activity-Relationships of 1H-Imidazo[4,5-c]quinolines That Induce Interferon Production, J. Med. Chem., 48 (2005) 3481-3491.
[40] G.H.M. Vondenhoff, S. Dubiley, K. Severinov, E. Lescrinier, J. Rozenski, A. Van Aerschot, Extended targeting potential and improved synthesis of Microcin C analogs as antibacterials, Bioorg. Med. Chem., 19 (2011) 5462-5467.
[41] A.D. Khoje, C. Charnock, B. Wan, S. Franzblau, L.-L. Gundersen, Synthesis and antimycobacterial activities of non-purine analogs of 6-aryl-9-benzylpurines: Imidazopyridines, pyrrolopyridines, benzimidazoles, and indoles, Bioorg. Med. Chem., 19 (2011) 3483-3491.
[42] A. Krajczyk, J. Zeidler, P. Januszczyk, S. Dawadi, H.I. Boshoff, C.E. Barry, 3rd, T. Ostrowski, C.C. Aldrich, 2-Aryl-8-aza-3-deazaadenosine analogues of 5'-O-[N-(salicyl)sulfamoyl]adenosine: Nucleoside antibiotics that block siderophore biosynthesis in Mycobacterium tuberculosis, Bioorg. Med. Chem., 24 (2016) 3133-3143.
[43] P. Chomczynski, N. Sacchi, The single-step method of RNA isolation by acid guanidinium thiocyanate-phenol-chloroform extraction: twenty-something years on, Nat. Protoc., 1 (2006) 581-585.
[44] R.A. Copeland, Tight Binding Inhibition, in: Evaluation of Enzyme Inhibitors in Drug Discovery, John Wiley & Sons, Inc., 2013, pp. 245-285.
[45] D. Xu, Y. Zhang, Ab Initio structure prediction for Escherichia coli: towards genome-wide protein structure modeling and fold assignment, Sci. Rep., 3 (2013) 1895.
[46] E.F. Pettersen, T.D. Goddard, C.C. Huang, G.S. Couch, D.M. Greenblatt, E.C. Meng, T.E. Ferrin, UCSF Chimera--a visualization system for exploratory research and analysis, J. Comput. Chem., 25 (2004) 1605-1612.
[47] K. Katoh, J. Rozewicki, K.D. Yamada, MAFFT online service: multiple sequence alignment, interactive sequence choice and visualization, Brief. Bioinform., (2017).
[48] A.M. Waterhouse, J.B. Procter, D.M. Martin, M. Clamp, G.J. Barton, Jalview Version 2--a multiple sequence alignment editor and analysis workbench, Bioinformatics, 25 (2009) 1189-1191.
[49] G.E. Crooks, G. Hon, J.M. Chandonia, S.E. Brenner, WebLogo: a sequence logo generator, Genome Res., 14 (2004) 1188-1190.

Figures and Legends:

A

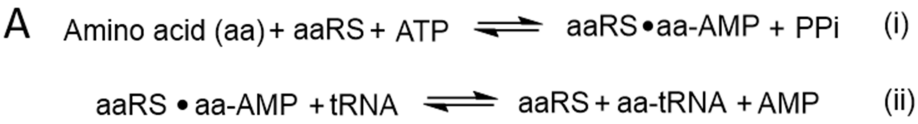

B

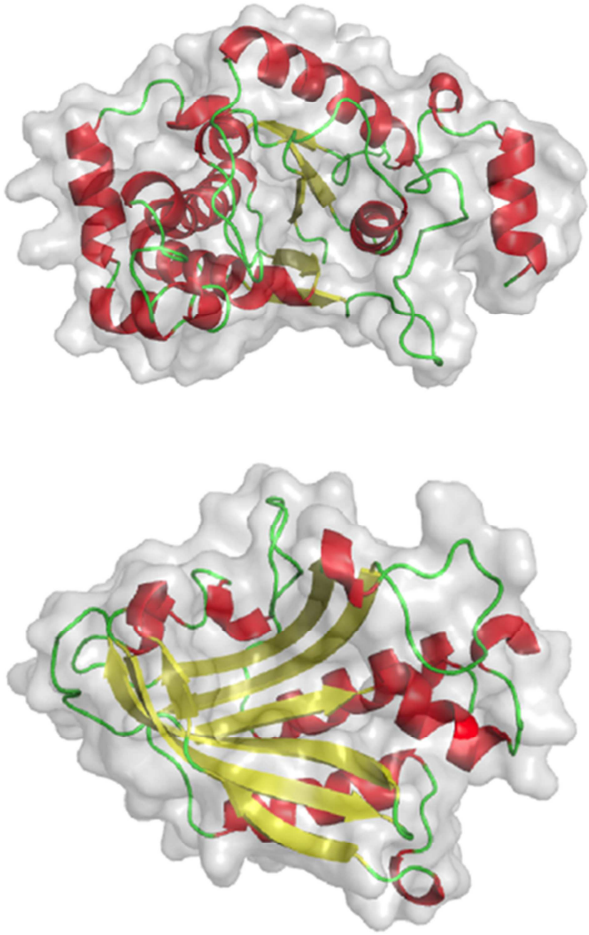

Figure 1. Activity and architecture of aaRS family members. (A) The two step reaction mechanism shared amongst all aaRS. (B) Architecture of the core catalytic domain of class I (upper) and class II (bottom) aaRS enzymes. Cartoon and surface representation of residues 1-222 of class I tyrosyl-tRNA synthetase (PDB:3TS1) and class II glycyl-tRNA synthetase α-subunit (PDB: 3UFG). For clarity only the monomeric subunit of each aaRS is shown.

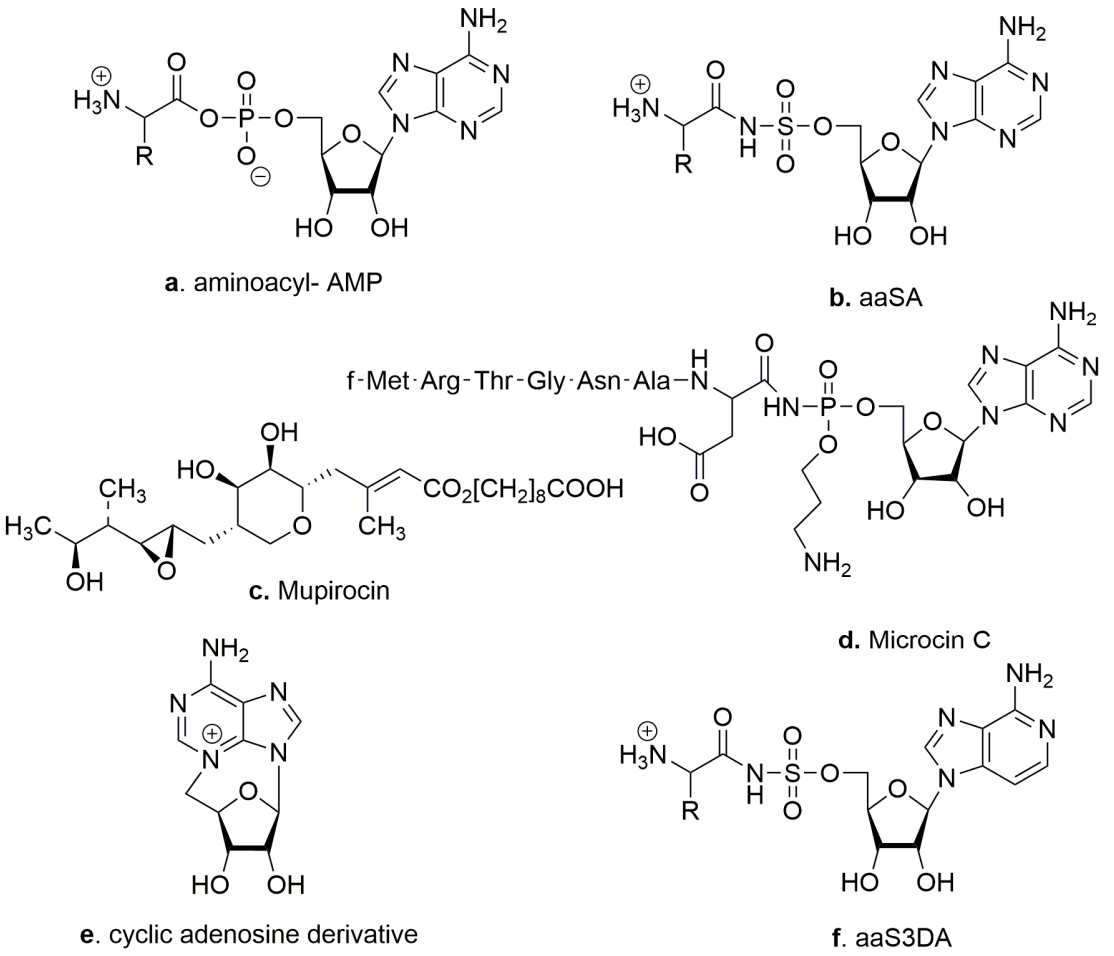

Figure 2. Chemical structures of aminoacyl-adenylate (**a**), aminoacyl-sulfamoyl adenosines (**b**), natural aaRS inhibitors (**c** and **d**), cyclized adenosine (**e**) and aminoacyl-sulfamoyl 3-deazaadenosines (**f**).

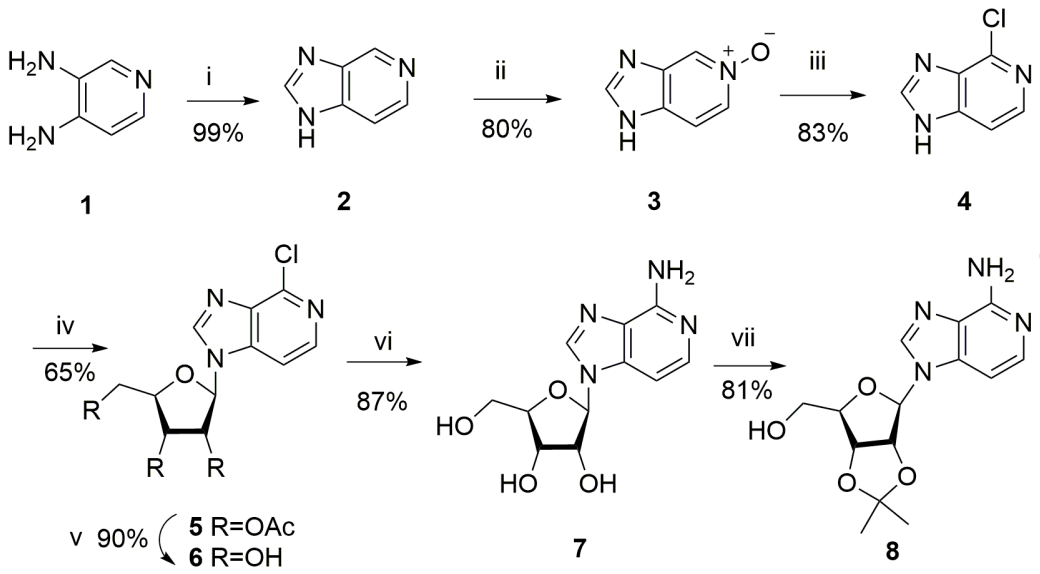

Scheme 1. Synthesis of 3-deazaadenosine. Reagents and conditions: (i) triethyl orthoformate, formic acid, 145 ℃, 6 h; (ii) m-CPBA, DCM/methanol (2:1), room temperature overnight; (iii) $POCl_3$, 120 ℃, 3 h; (iv) 1',2',3',5'-tetra-*O*-acetyl-β-D-ribofuranose, $SnCl_4$, dry acetonitrile, room temperature 24 h; (v) 7 N ammonia in methanol, 0 ℃ to rt., 1 h; (vi) a) hydrazine hydrate, 120 ℃, 6-8 h b) Raney Ni, 120 ℃, 30 min; (viii) p-TSA, dry acetone, DMP, rt, 3h.

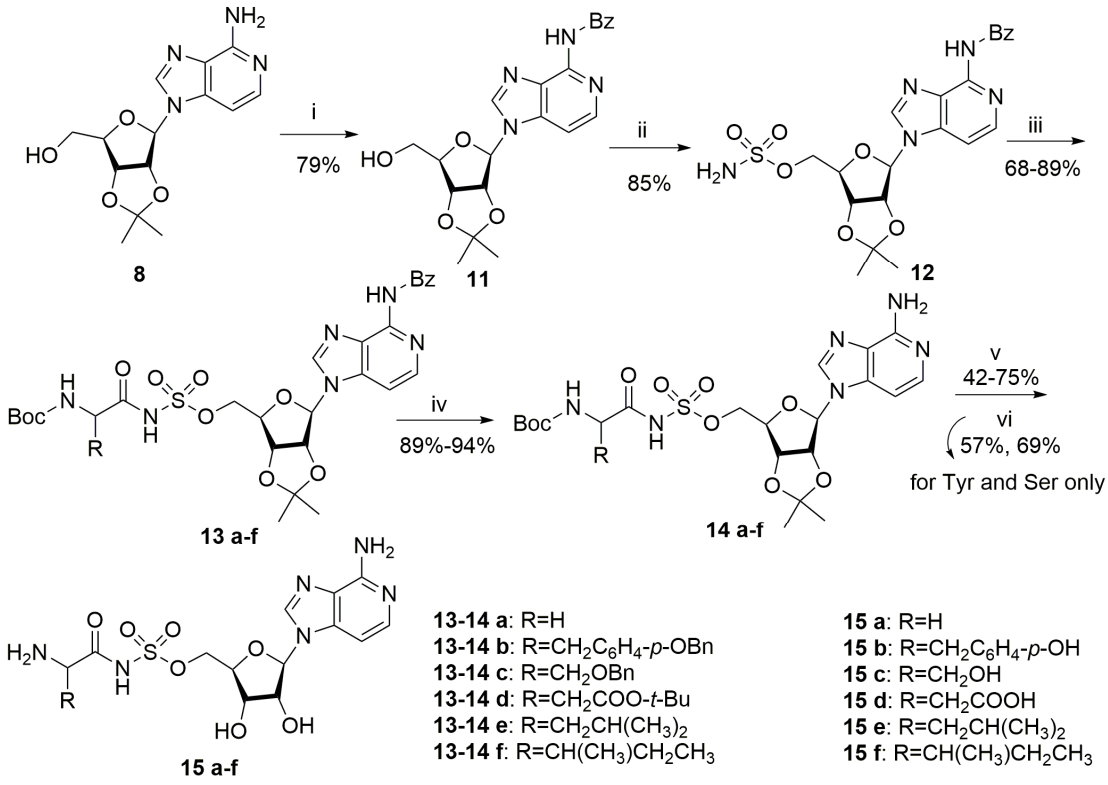

Scheme 2. Synthesis of aminoacyl-sulfamoyl aaS3DA derivatives. Regents and conditions: (i) a) TMSCl, b) BzCl, c) 12% aqueous ammonia, 0 □ to r.t, 6-8 h; (ii) NH_2SO_2Cl, acetonitrile, room temperature overnight; (iii) N-Boc-aa-(tBu/Bn)-OSu, DBU, dry DMF, room temperature overnight; (iv) sodium methoxide, methanol, reflux, 2 h; (v) TFA/H_2O, 5:2 (v/v), 3h; (vi) Pd/C, methanol, H_2 atm. room temperature overnight.

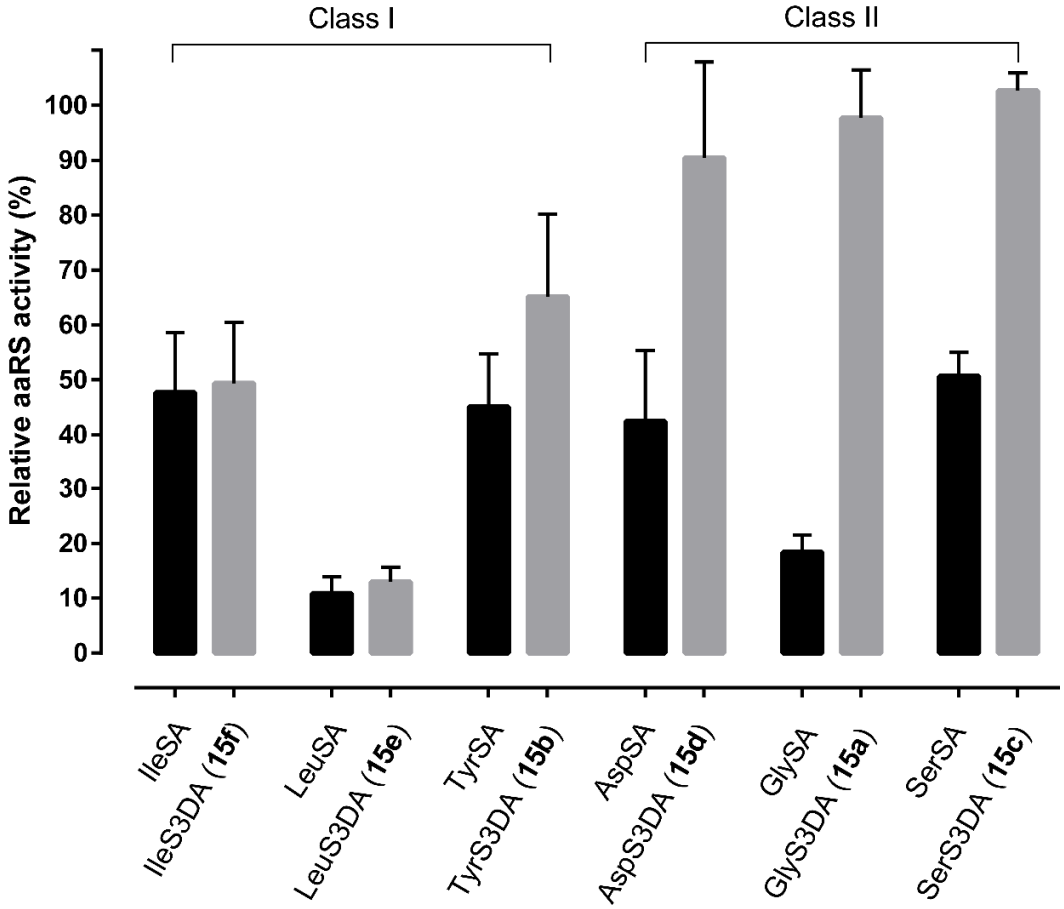

Figure 3. Comparative inhibitory activity of the aaSA (black bars) and the aaS3DA analogues (grey bars) in *E. coli* K-12 BW28357 strain S30 extracts. Activity was determined by measuring the transfer of the appropriate ^{14}C-labelled amino acid to tRNA in the presence of 2.5 µM of each compound. The relative activity was determined by comparing to values measured in the absence of any compound and assuming 100% enzyme activity. Average of three experiments, with SD error bar.

Table 1. K_i^{app} of aaSA and the aaS3DA analogues, where aa is the corresponding amino acid. Values were determined from fitting the dose response curve for each compound with the Greco-Hakala equation. Units are in nanomolar (nm).

	AaRS	aaSA		aaS3DA	
		K_i^{app}	E_0	K_i^{app}	E_0
Class I	**IleRS**	1.92 ± 4.0	141 ± 19	213 ± 40	141 ± 80
	LeuRS	0.139 ± 0.10	1.24 ± 0.31	0.654 ± 0.082	0.533 ± 0.21
	TyrRS	2.93 ± 1.2	6.23 ± 2.6	29.9 ± 14.8	15.2 ± 28.7
Class II	**AspRS**	0.052± 0.04	1.19 ± 1.60	25.3 ± 5.3	1.41 ± 11.7
	GlyRS	148 ± 48	62 ± 97	> 2000	/
	SerRS	0.18± 0.07	0.75 ± 0.16	522.5 ± 33.2	2.52 ± 6.8

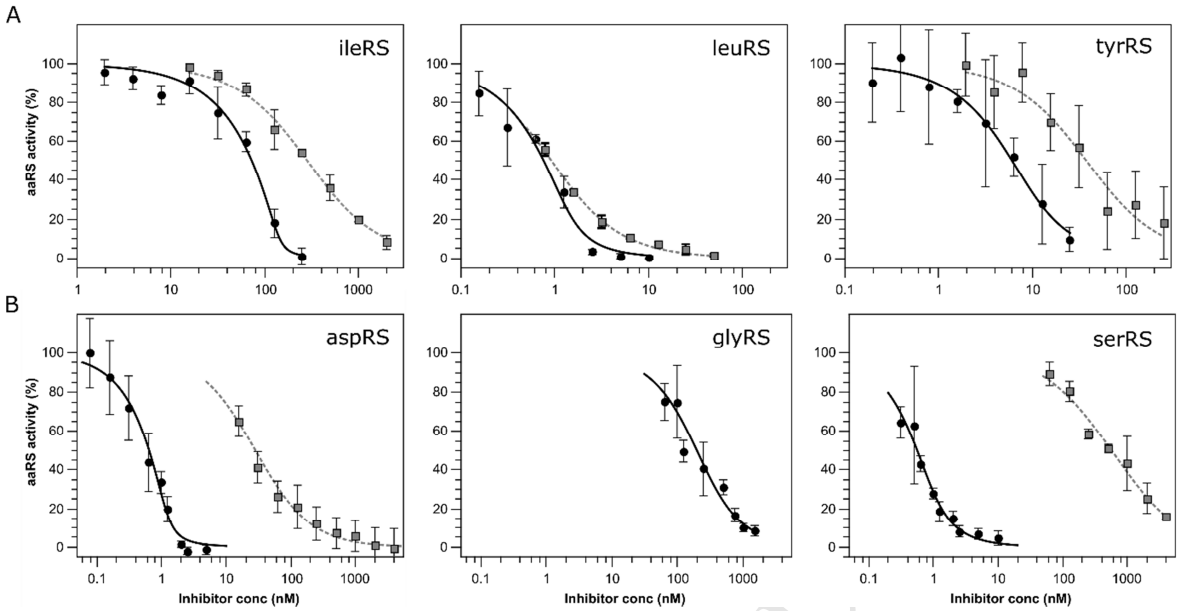

Figure 4. Dose response curves of purified E. coli aaRS in the presence of aaSA (black circles, black line) or aaS3DA (grey boxes, grey dashed line). The activity of each enzyme is reported as a percentage value relative to that measured in the absence of inhibitor. (A) Class I enzymes (B) Class II enzymes. The presented fit of the measured points was calculated using the Greco-Hakala equation for high affinity binders.

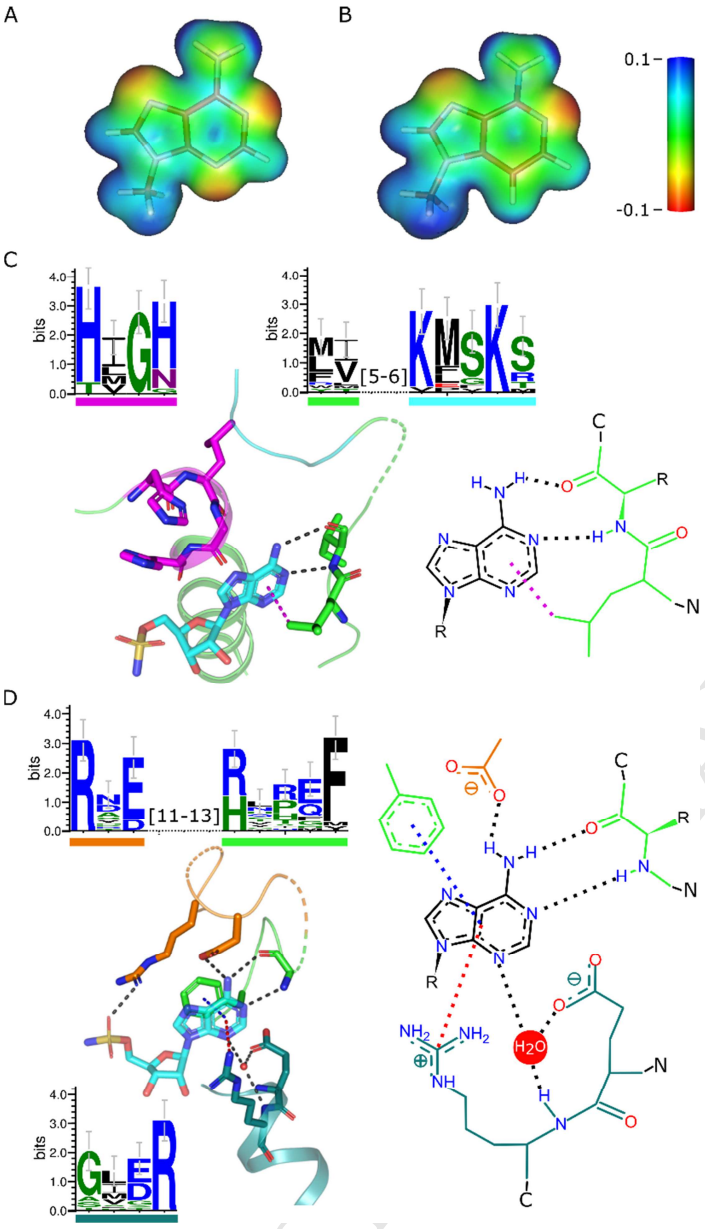

Figure 5. Computational chemistry and bioinformatics analyses. QM calculations of the electrostatic potential of (A) 9-methyl-adenine and (B) 9-methyl-3-deazaadenine, calculated at the MP2/6-31G** level, mapped onto the electron density. The spectrum bar in panel B corresponds to the mapped potential for both compounds.A stick representation of each compound, within the isodensity, is also shown. Structure and sequence conservation of observed base interactions present in Class I (C) and Class II (D) aaRS. For each class a representative structure was identified in the PDB bound to an aaSA. The backbone of the essential structural elements are depicted as a cartoon, with residues making key interactions represented as sticks. An observed water molecule observed in class II aaRS is shown as a red sphere. An equivalent 2D representation of the interactions, using the same colouring is also shown. Identified H-bonds, cation-π, π-π and π-σ interactions are presented as black, red, blue and magenta dashed lines, respectively. The conservation of key residues for base recognition, identified from a structural alignment of *E. coli* and *S. aureus* Class I and Class II aaRS orthologues are shown as sequence logos. The

numbers in each logo correspond to the number of non-conserved residues observed in the structural alignment that separate the identified motifs. In both structural representations participating residues are coloured according to the conserved motifs they are part of, represented as an equivalently coloured bar under each sequence logo.

Research Highlights:

- Six new aminoacyl-sulfamoyl-3-deazaadenosine (aaS3DA) derivatives were prepared
- These proved to be inhibitors of aminoacyl-tRNA synthetases (aaRS)
- aaS3DA and aaSA analogues targeting class I enzymes display about equal inhibition
- Removal of the N^3 position of aaSAs proved detrimental for class II aaRS enzymes